

MEASUREMENT OF HEAT TRANSFER COEFFICIENT
OF A FALLING LIQUID FILM

A THESIS

SUBMITTED TO THE DEPARTMENT OF CHEMICAL ENGINEERING
IN PARTIAL FULFILMENT OF THE REQUIREMENTS
FOR THE DEGREE OF
MASTER OF SCIENCE IN ENGINEERING(CHEMICAL)

BY

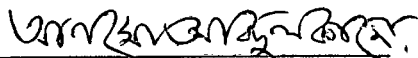
GOPAL CHANDRA PAUL



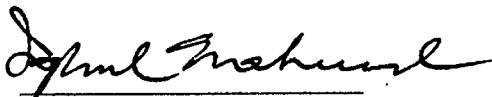
BANGLADESH UNIVERSITY OF ENGINEERING AND TECHNOLOGY, DHAKA
MAY, 1988

BANGLADESH UNIVERSITY OF ENGINEERING AND TECHNOLOGY
DEPARTMENT OF CHEMICAL ENGINEERING
CERTIFICATION OF THESIS WORK

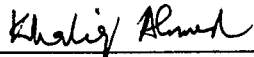
We, the undersigned, certify that GOPAL CHANDRA PAUL candidate for degree of Master of Science in Engineering (Chemical) has presented his thesis on the subject "MEASUREMENT OF HEAT TRANSFER COEFFICIENT OF A FALLING LIQUID FILM" that the thesis is acceptable in form and content, and that the student demonstrated a satisfactory knowledge of the field covered by this thesis in an oral examination held on the 7th May, 1988.



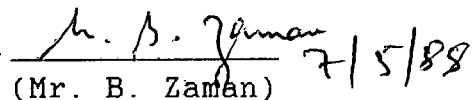
(Dr. A.K.M.A. Quader)
Professor
Department of Chemical Engineering
Chairman, Examination Committee.



(Dr. Iqbal Mahmud)
Professor
Department of Chemical Engineering
Member, Examination Committee.



(Dr. Khaliq Ahmed)
Assistant Professor
Department of Chemical Engineering
Member, Examination Committee.

 7/5/88

(Mr. B. Zaman)
Senior General Manager
R & PD, Bangladesh Chemical Industries Corporation,
BCIC Building, 30-31 Dilkusha C/A, Dhaka.
External Member, Examination Committee.

ABSTRACT

An experimental investigation was undertaken to measure the heat transfer coefficients of falling liquid films. The measurements were carried out using a double-pipe vertical heat exchanger. The inside tube was a smooth 304-stainless steel tube, 2 m long and 2.54 cm I.D. Experimental fluids were urea solutions having concentration ranging from 10 to 60% by weight. Saturated steam was used as the heating medium. Wall temperatures were measured with thermocouples embedded into the outside wall at equal distances along the tube. Heat balances checked within $\pm 10\%$.

The h - T plots for urea solutions show lower heat transfer coefficients with the increase of concentration of urea in water. but on h - Re plots, it was observed that at any Re heat transfer coefficients are independent of concentrations upto 30% and increase as the concentrations increase thereafter.

The heat transfer results were correlated by employing dimensionless groups such as Nu , Re and Pr and the resultant correlation obtained is:

$$Nu = 4.3 \times 10^{-6} Re^{1.3} Pr^{1.71}$$

The experimental data were correlated with a standard deviation of $\pm 9.0\%$.

All physical properties data were evaluated at the average bulk temperature and 78% data were in the laminar regime.

ACKNOWLEDGEMENT

The author would like to express his gratitude to the following:

Prof. A.K.M.A. Quader for his constant encouragement, guidance and supervision and providing sufficient facilities throughout the work.

Prof. Jasimuz Zaman and Prof. Khaliqur Rahman for their encouragement and thoughtful suggestions.

Mr. Mollah Ahmed Ali of the central workshop for his cooperation during the fabrication of the heat exchanger.

Laboratory technicians of the Department of Chemical Engineering for their help in setting up of the experimental rig.

His wife, Mrs. Kamana Rani Paul, for her encouragement and patience during this work.

His friends and colleagues, Mr. M.A. Muqeem and Edmond Gomes for their help during this work.

CONTENTS

	<u>page</u>
ABSTRACT	(i)
ACKNOWLEDGEMENT	(ii)
CONTENTS	(iii)
CHAPTER 1 <u>INTRODUCTION</u>	1
CHAPTER 2 <u>LITERATURE REVIEW</u>	3
2.1 Introduction	3
2.2 Hydrodynamics	3
2.2.1 Laminar Flow	3
2.2.2 Laminar Flow with Interfacial Shear	7
2.2.3 Laminar Flow with Rippling	9
2.2.4 Turbulent Flow	11
2.2.5 Turbulent Flow with an adjoining gas stream	13
2.3 Heat Transfer	13
2.3.1 Heat Transfer in Laminar Flow	14
2.3.2 Heat Transfer with Turbulent Flow	17
2.3.3 Empirical Correlation	20
2.3.3.1 Laminar Flow	20
2.3.3.2 Turbulent Flow	22
CHAPTER 3 <u>OBJECTIVES OF THE WORK</u>	26
CHAPTER 4 <u>EXPERIMENTAL EQUIPMENT AND EXPERIMENTAL</u> <u>PROCEDURE</u>	27
4.1 Introduction	27
4.2 Experimental Equipment	27
4.3 Experimental Procedure	35
4.4 Measurement of Thermal Conductivity	36

	<u>page</u>
CHAPTER 5 <u>EXPERIMENTAL RESULTS</u>	39
5.1 Proof of Experimental Procedure	39
5.2 Experimental Fluids and their Physical and Thermal Properties	39
5.3 Presentation of Experimental Results	41
5.4 Analysis of Experimental Results	43
CHAPTER 6 <u>DISCUSSIONS OF THE RESULTS</u>	45
6.1 The h-Γ plots for water	45
6.2 The h-Re plots for water	46
6.3 The h-Γ plots for urea solutions	46
6.4 The h-Re plots for urea solutions	47
6.5 Correlation of Heat Transfer Results	48
CHAPTER 7 <u>CONCLUSIONS</u>	51
CHAPTER 8 <u>RECOMMANDATIONS FOR FUTURE WORK</u>	52
NOMENCLATURE	53
REFERENCES	56
<u>APPENDIX A</u> TABLES	59
Table 5.1a. Heat Transfer Data for Water	60
Table 5.1b Calculated Results for Water	62
Table 5.5a Heat Transfer Data for Urea solutions	63
Table 5.5b Calculated Results for Urea solutions	71
Table 5.6 Comparison of Experimental Coefficients with those from Eqs. (2.74) and (2.76)	76

	<u>page</u>
<u>APPENDIX B</u> FIGURES	81
Figure 5.1 Film Heat Transfer Coefficient vs. Mass Flow Rate per unit width of the tube for water	82
Figure 5.2 Film Heat Transfer Coefficient vs. Reynolds number for water	83
Figure 5.3 Film Heat Transfer Coefficient vs. Mass Flow Rate per unit width of the tube for urea solutions	84
Figure 5.4 Film Heat Transfer Coefficient vs. Reynolds number for urea solutions	85
Figure 5.5 $Nu_{\text{expt}}/Pr^{1.7082}$ vs. Reynolds number	86
Figure 5.6 Experimental Nusselt number vs. Calculated Nusselt number	87
<u>APPENDIX C</u> COMPUTER PROGRAM LISTINGS	88

CHAPTER 1

INTRODUCTION

Falling film heat exchangers are frequently encountered in a number of processing industries including food. The fluid enters at the top of the vertical tubes and is distributed on the inside surface of the tubes in the form of film through distributors. The film can be cooled, heated or evaporated with suitable heat transfer medium from the outside of the tubes.

Principal advantages of such heat transfer arrangement are: high rate of heat transfer, no internal pressure drop, short time of contact (very important for heat sensitive materials) and easy accessibility to tube for cleaning.

A study of report on "Urea, Its Properties and Manufacture" made by Chao[11], the pilot plant work by Young and Sinek[40] and the report of Herbert and Sterns[22] indicated that design methods are by no means satisfactory. The particular problem being experienced is the unsatisfactory distribution of the fluid as a film at the top of the tube. Limited work has been published on the actual measurements of heat transfer coefficients in falling films of liquid inside vertical tubes on the fluids having industrial interest.

In the course of processing liquids, particularly heating in a falling film heat exchanger, it is important to understand the problems of heat transfer to liquids in such exchangers. The

knowledge of heat transfer coefficient of a falling liquid film is required by the designers concerned with the sizing of exchanger and evaluation of its performance.

This work investigates experimentally the heat transfer characteristics of water and aqueous solution of urea with concentrations ranging from 10 to 60% by weight in a vertical double-pipe heat exchanger. The heat transfer coefficient depends on the film flow rate, concentration of solute in liquid and the physical properties of the liquid. The experimental data are empirically correlated with dimensionless groups.

CHAPTER 2

LITERATURE REVIEW2.1 INTRODUCTION

The flow of thin films under the influence of gravity is commonly encountered in many chemical process industries during heat and mass transfer. The prediction of flow rate, heat and mass transfer relationships are perhaps the most common problems. In such processes momentum, heat and mass transfers are intimately connected. Flow regimes include: laminar, transition and turbulent.

2.2 HYDRODYNAMICS

Hydrodynamics of flowing liquid films is of importance in a wide range of practical problems involving film flow. Such problems include the calculation of heat transfer in heat exchangers, evaporators and condensers; and mass transfer in film type equipment. In this section the general equations are set up, and the important results of the various treatments of smooth laminar flow, wavy flow, turbulent flow and flow of films with an adjoining gas stream will be discussed in brief. An excellent review has been presented by Fulford[19] encompassing different types and aspects of film flow.

2.2.1 LAMINAR FLOW

The most general equation for laminar flow of a various incompressible fluid of constant physical properties is the Navier-Stokes equation given below.

$$\rho \frac{DU}{Dt} = -\nabla P + \mu \nabla^2 U + \rho g \quad (2.1)$$

In addition the equation of continuity

$$\nabla \cdot U = 0 \quad (2.2)$$

must be satisfied.

Consider the flow of a falling film of a Newtonian fluid along a vertical flat plate as shown in Figure 2.1. For this system the following assumptions are made[7]:

- (1) The flow is laminar and incompressible (Re less than about 2100).
- (2) The density is constant.
- (3) The flow is independent of time (steady state).
- (4) End effects are neglected.
- (5) The fluid behaves as a continuum.
- (6) There is no slip at the wall.
- (7) There is no drag at the gas-liquid interface.

On the basis of these assumptions Eqs. (2.1) and (2.2) reduce to the very simple case originally obtained by Nusselt[34].

$$\frac{d^2 u_z}{dy^2} + \frac{\rho g}{\mu} = 0 \quad (2.3)$$

$$\frac{dp}{dy} = \rho g \quad (2.4)$$

$$\frac{dp}{dz} = 0 \quad (2.5)$$

$$\frac{du_z}{dz} = 0 \quad (2.6)$$

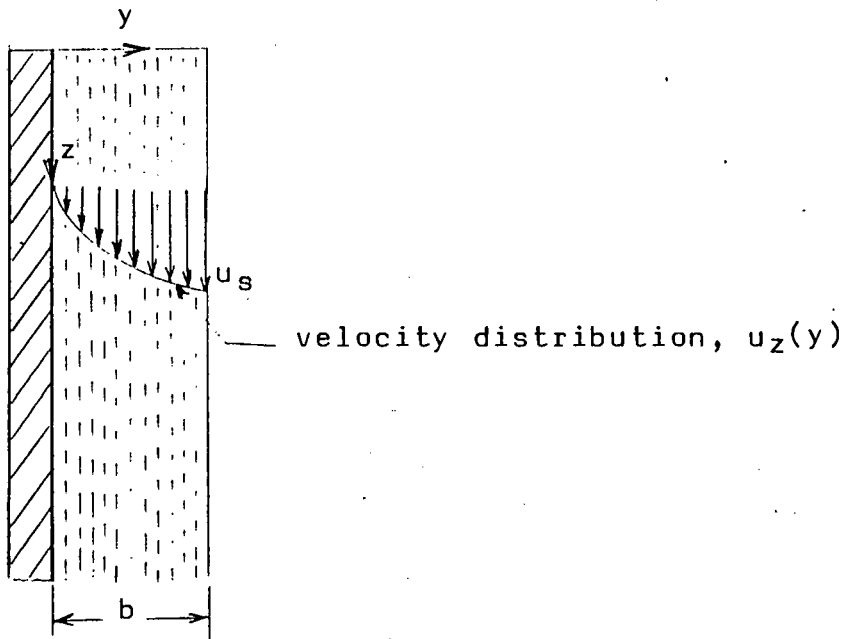


Figure 2.1 Laminar flow of a liquid film along a vertical flat plate

The boundary conditions to be satisfied are:

$$u_z = 0 \text{ at } y=0 \text{ (no slip at wall)}$$

$$\frac{du_z}{dy} = 0 \text{ at } y=b \text{ (no drag at interface)}$$

the velocity distribution is given by the semiparabolic equation

$$u_z = \frac{\rho g b^2}{2\mu} \left[\frac{2y}{b} - \left(\frac{y}{b} \right)^2 \right] \quad (2.7)$$

The surface velocity (at $y=b$) is, therefore,

$$u_s = \frac{\rho g b^2}{2\mu} \quad (2.8)$$

By integrating Eq.(2.7) over the film thickness, the mean velocity is found to be

$$\bar{u} = \frac{\rho g b^2}{3\mu} \quad (2.9)$$

$$\text{where, } u_s / \bar{u} = 1.5 \quad (2.10)$$

The mass flow rate per wetted perimeter is

$$\Gamma = \rho b \bar{u} = \frac{\rho^2 g b^3}{3\mu} \quad (2.11)$$

In absence of drag at the surface, the wall shear stress must support the total body force on the film, so that

$$\tau_w = \rho b g = (3 \rho \mu g^2 \Gamma)^{1/3} \quad (2.12)$$

Using the film Reynolds number defined as

$$Re = \frac{4 \rho \bar{u} b}{\mu} = \frac{4 \Gamma}{\mu} \quad (2.13)$$

the results presented above can be re-written to give:

$$\bar{u} = \left(\frac{\mu g}{48 \rho} \right)^{1/3} Re^{2/3} \quad (2.14)$$

$$b = \left(\frac{3 \mu^2}{4 \rho^2 g} \right)^{1/3} Re^{1/3} \quad (2.15)$$

$$\tau_w = \left(\frac{3 \rho \mu^2 g^2}{4} \right)^{1/3} Re^{1/3} \quad (2.16)$$

If the friction factor for the film is defined in the usual way of Fanning, so that $f = \frac{\tau_w}{\frac{1}{2} \rho u^2}$, then by substituting for τ_w and u from Eq.(2.16) and (2.14), one would get

$$f = \frac{24}{Re} \quad (2.17)$$

which can be compared with the analogous value for laminar flow in closed conduits,

$$f = \frac{16}{Re} \quad (2.18)$$

When the film flows on a vertical cylindrical surface of radius R as shown in Figure 2.2, Eq.(2.3) becomes

$$\frac{d^2 u_z}{dr^2} + \frac{1}{r} \frac{du_z}{dr} + \frac{\rho g}{\mu} = 0 \quad (2.19)$$

with r as the radial coordinate, which is to be solved with the boundary conditions

$$u_z = 0 \text{ at } r = R \text{ (no slip at tube wall)}$$

$$\frac{du_z}{dr} = 0 \text{ at } r = R-b \text{ (no drag at interface)}$$

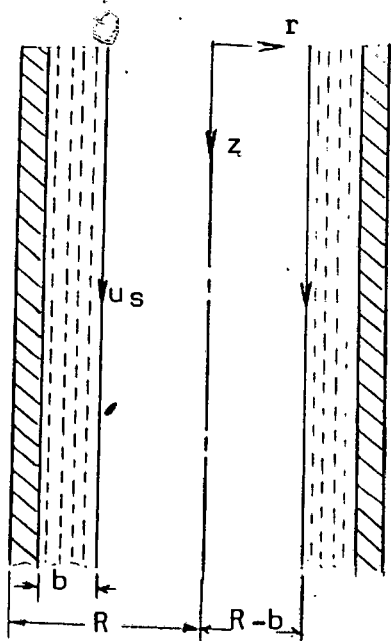


Figure 2.2 Laminar flow of a liquid film on inside of a vertical cylindrical tube

The velocity profile is found to be

$$u_z = \frac{\rho g}{4\mu} (R^2 - r^2) + \frac{\rho g(R-b)^2}{2\mu} \ln(r/R) \quad (2.20)$$

and the mass flow rate per wetted perimeter is

$$\Gamma = \frac{\rho^2 g}{4\mu} \left[\frac{(R-b)^4}{R} \ln \frac{R}{R-b} + \frac{3(R-b)^4}{4R} - R(R-b)^2 + \frac{R^3}{4} \right] \quad (2.21)$$

By expanding the terms above in powers of \$(b/R)\$ one should obtain

$$\Gamma = \frac{\rho^2 g b^3}{3\mu} \left[1 - \frac{b}{R} + \frac{3}{20} \left(\frac{b}{R} \right)^2 + \frac{1}{40} \left(\frac{b}{R} \right)^3 \dots \right] \quad (2.22)$$

This is the most general case of equation. As the tube radius \$R\$ tends to infinity, Eq.(2.22) reduces to Eq.(2.11), that is, the case of a vertical flat plate is obtained.

2.2.2 LAMINAR FLOW WITH INTERFACIAL SHEAR

For smooth laminar film flow with an interfacial shear the equations of motions remains the same as shown in Eq.(2.1), but the boundary condition $\frac{du_z}{dy} = 0$ at \$y = b\$ must be replaced by [12]

$$\left(\frac{du_z}{dy} \right)_{y=b} = -\tau_i / \mu \quad (2.23)$$

with τ_i as the interfacial shear, in which case

$$u_x = \frac{\rho g b^2}{2\mu} \left[-\frac{2y}{b} - \left(\frac{y}{b} \right)^2 \right] - \frac{\tau_i y}{b} \quad (2.24)$$

Semenov[35] considered the case of smooth film flow with an interfacial shear τ_i (which may be either positive or negative) and a pressure drop in the gas stream of Ψ . Semenov's expression for the volumetric flow per wetted perimeter was

$$Q = \left(\frac{\rho g - \Psi}{3\mu} \right) b^3 - \frac{\tau_i b^2}{2\mu} \quad (2.25)$$

At the commencement of flooding in a wetted wall column, the net flow is zero ($Q=0$), and, with this value, various solutions of Eq.(2.25) can be studied. With τ_i positive countercurrent flow, flooding commences at a film thickness of

$$b = \frac{3 \tau_i}{2(\rho g - \Psi)} \quad (2.26)$$

More recently, Brauer[9] carried out a detailed analysis of the flow of smooth films and gas streams inside vertical tube, this work subsequently extended by Feind[17]. In this treatment all possible cases of film/gas flow(countercurrent, upward cocurrent, and downward cocurrent) are dealt in a unified manner by plotting the calculated results in the form of $|f|$ as a function of Re_{gas} . $|f|$ is expressed as

$$|f| = \frac{2 \tau_i}{\rho_{gas} (\bar{u}_{gas})^2} = \frac{2(\Delta p)(R-b)}{\rho_{gas} (\bar{u}_{gas})^2 L} \quad (2.27)$$

where $\Delta p/L$ is the pressure drop per unit length of wetted tube. The gas stream Reynolds number is defined as

$$Re_{gas} = \frac{2 \rho_{gas} (R-b) \bar{u}_{gas}}{\mu_{gas}} \quad (2.28)$$

Feind[17] has shown that the effect of an interfacial shear τ_i due to a countercurrent gas stream is to increase the film thickness in the ratio

$$\frac{b}{b_0} = \left(1 - \frac{3\tau_i}{2\rho bg}\right)^{-1/3} \quad (2.29)$$

where b_0 denotes the value in absence of a gas stream. Flooding commences when

$$\frac{\tau_i}{\rho bg} = \frac{2}{3} \quad (2.30)$$

It is found that the ratio of the wall shear stresses τ_w/τ_{w0} decreases with $\tau_i/\rho bg = 1/2$ and then increases sharply. The surface velocity in the presence of gas stream is shown to be

$$u_w = \frac{\rho gb^2}{\mu} \left(\frac{1}{2} - \frac{\tau_i}{\rho bg} \right) \quad (2.31)$$

and it can be deduced that the ratio of the surface velocity to the mean velocity of the film is given by

$$\frac{u_w}{\bar{u}} = 3 \left(1 - \frac{2\tau_i}{\rho bg}\right) / \left(2 - \frac{3\tau_i}{\rho bg}\right) \quad (2.32)$$

which reduces to the value given by Eq.(2.11) if $\tau_i = 0$.

It is to be noted that these treatments assume that the pressure drop per unit length is constant over the length of the wetted tube and that the film is in smooth laminar flow, which is usually the case only at very low flow rates.

2.2.3 LAMINAR FLOW WITH RIPPLING

Only the slowest films are free from waves. Long before the flow becomes turbulent, waves are found on the films. The critical Reynolds number for the onset of wave for films of water

was measured by Kirkbride[27] as 8, Friedman and Miller[18] as 24, Grimley[21] as 24 and Binne[6] as 17.6. According to Jackson[25] the onset of wave is independent of Reynolds number, being a function of Froude number only. However, for parabolic flow in a gas-liquid system $Re = 12 Fr$. His experiment gives $Fr = 1$, i.e., $Re = 12$.

Theoretical work of Yih[39] estimates the critical Reynolds number to be 6 and it is independent of the nature of the fluids. Kapitza[26] expresses Re_{cr} as

$$Re_{cr} = 2.44 \left(\frac{\rho \sigma^3}{\mu^4 g} \right)^{1/11} \quad (2.33)$$

Brooke-Benjamin[10] who argues that there is no critical Reynolds number, since waves are amplified under all conditions. As a wave travels 10 cm. down a vertical plane the amplification is given by

$$A = \exp(0.0571 Z Re^{7/3}) \quad (2.34)$$

$$\text{where, } Z = \rho/\mu(g\mu/\rho)^{2/3}$$

This equation is of such form that A is nearly 1 for Re less than a certain value and rapidly becomes large for Re greater than that value. Brooke-Benjamin defines this value as the quasi-critical Reynolds number, Re_{qc} , that is the Reynolds number above which waves become noticeable on a plane of finite size. Like Re_{cr} , this is a function of surface tension and viscosity. For water at room temperature Re_{qc} is about 16.

2.2.4 TURBULENT FLOW

The problem of turbulent flow in thin films has received comparatively little attention, because of the great complexity of the flow processes involved. There are no theoretical treatments of the problems of wavy turbulent flow, and the usual procedure is to neglect the surface waves and to obtain solutions for the case of smooth turbulent flow.

For fully developed turbulent flow with zero interfacial shear ($\tau_i = 0$), it has been shown [28,29] that the mean film velocity is

$$\bar{u} = \sqrt{\frac{y_b}{K}} \ln \left(\frac{\rho b}{\mu} \sqrt{\frac{y_b}{K}} \right) \quad (2.35)$$

where K is a constant. No numerical value is given for K , but substitution of the value $b=0.076$ cm. for $Re=4,000$ obtained experimentally [8] for a water film ($\mu/\rho = 0.01$ cm²/sec) on a vertical wall shows that K should be in the region of $1/9$.

Nearly all of the remaining treatments of turbulent film flow are based on the assumption that the film can be regarded as smooth, and that some form of the dimensionless velocity profile valid for single phase flow (pipe flow) can be applied to the film flow. In principle the treatments differ mainly in the form of the dimensionless velocity profile. The universal velocity profile equations used by Dukler and Bergelin [15] are as follows:

$$u^+ = y^+ \quad \text{for } 0 < y^+ \leq 5 \text{ (laminar sublayer)} \quad (2.37)$$

$$u^+ = -3.05 + 5.0 \ln y^+ \quad \text{for } 5 < y^+ \leq 30 \text{ (buffer layer)} \quad (2.38)$$

$$u^+ = 5.5 + 2.5 \ln y^+ \quad \text{for } 30 < y^+ \leq b^+ \text{ (turbulent zone)} \quad (2.39)$$

where

$$u^+ = u_z / u^* \text{ (dimensionless velocity)} \quad (2.40)$$

$$y^+ = \rho y u^* / \mu \text{ (dimensionless distance from wall)} \quad (2.41)$$

$$b^+ = \rho b u^* / \mu \text{ (dimensionless film thickness)} \quad (2.42)$$

$$u^* = (\tau_w/\rho)^{1/2} \text{ (friction velocity)} \quad (2.43)$$

By integrating the dimensionless velocity over the film thickness, it is found for the case of turbulent flow ($b^+ \geq 30$) that

$$Re = b^+(12.0 + 10.0 \ln b^+) - 256 \quad (2.44)$$

In the case of zero interfacial shear the wall shear stress is given by Eq.(2.13). So from Eqs.(2.42) and 2.43) one obtains

$$b^+ = (g^{1/2} \rho) b^{3/2} / \mu \quad (2.45)$$

Hence knowing the values of the physical properties appearing in Eq.(2.45), it is possible to calculate the values of b for any value of Re using Eqs. (2.44) and (2.45).

In the case of flow of film in a tube of radius R , with a pressure drop of ψ per unit length, a force balance show that τ_w may be approximately expressed as

$$\tau_w = (\rho_{gas} g + \psi) R/2 + \rho b g \quad (2.46)$$

in place of Eq.(2.45), and in this case a trial and error or graphical solution is necessary in order to find b at a given Re and ψ .

According to this theory, the film becomes turbulent when $b^+ = 30$. Substituting of this value into Eq.(2.44) gives

$$Re_{cr} = 1080 \quad (2.47)$$

This result has been criticized[8] on the ground that recent investigations do not support the view of well-defined zones within the boundary layer.

2.2.5 TURBULENT FLOW WITH AN ADJOINING GAS STREAM

Dukler[16] has carried out an analysis of film flow based on the dimensionless velocity profile of Deissler[14], which includes the effect of a cocurrent downward gas stream. The analysis of Dukler was later extended to cover the case of upward cocurrent gas/film flow by Hewitt[29].

In their analysis a force balance is carried out on an element of the film, taking into account the gas shear on the interface, which is expressed in terms of the pressure drop per unit length in the gas stream (assumed constant). The interface is assumed to be smooth. In this way an expression is obtained for the shear stress distribution in the film, and this is converted to the dimensionless velocity profiles proposed for channel flow by Deissler[14] in the zone $0 < y^+ \leq 20$ and by von Karman[37] for the zone $y^+ > 20$. The equations obtained in this way were solved on a computer, and the numerical results have been presented graphically and in tabular form[16,23].

An important result of this treatment is that the dimensionless velocity u^+ within the film is no longer a unique function of the dimensionless distance from the wall, as in the single phase pipe flow, but depends significantly on a parameter involving the interfacial shear.

2.3 HEAT TRANSFER

Various aspects of heat transfer in laminar and turbulent liquid films, with and without evaporation have been treated. The solution of basic equations for heat transfer in falling films are similarly treated but the techniques are far from being satisfactory. Various empirical correlations available are also presented in this section.

2.3.1 HEAT TRANSFER IN LAMINAR FLOW

Heat transfer in fluids rarely involves a single mechanism but usually a combination of more than one mechanism. The analysis of heat transfer problems does not necessarily require that all parts shall be solved with equal care. Once the problem and the most important factors affecting the heat transfer mechanism have been identified some minor effects can be ignored. A complete solution of the momentum, mass and energy equations gives the temperature distribution in the fluid. For engineering applications, all such solutions involving readily measurable thermal and physical properties, pipe dimensions, flow rates etc. are useful. The heat transfer coefficients are dependent on the boundary conditions and the other phenomena involved in the problems such as (a) entry conditions, (b) wall conditions, (c) natural convection effects and (d) variations of physical and thermal properties.

The energy equation for a fluid flowing in a circular pipe in laminar motion as shown in Figure 2.3 may be written in the form

$$u_z \frac{\delta T}{\delta z} = \frac{k}{\rho c_p} \left[\frac{1}{r} \frac{\delta}{\delta r} \left(r \frac{\delta T}{\delta r} \right) + \frac{\delta^2 T}{\delta z^2} \right] + \frac{\mu}{\rho c_p} \left[2 \left(\frac{\delta u_z}{\delta z} \right)^2 + \left(\frac{\delta u_z}{\delta r} \right)^2 \right] \quad (2.48)$$

It is convenient to discuss the subject of heat transfer in laminar liquid films in terms of a two dimensional films, that is, a film on an infinite vertical plane. The use of solution of this type is often accurate enough for films on the outside or inside of vertical round tubes, provided that the tube diameter is not too small. The two-dimensional heat transfer equation in rectangular coordinates can be written as follows:

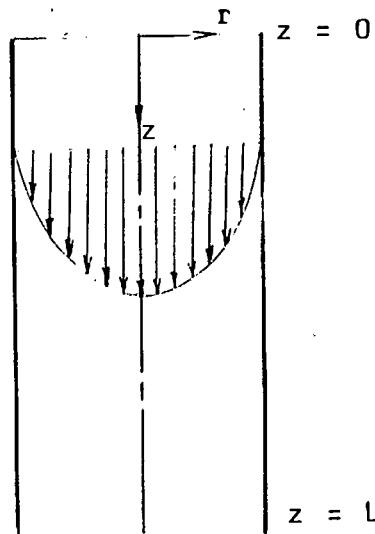


Figure 2.3 Laminar flow of liquid in vertical circular tube

$$u_z \frac{\delta T}{\delta z} = \frac{k}{\rho c_p} \left[\frac{\delta^2 T}{\delta y^2} + \frac{\delta^2 T}{\delta z^2} \right] + \frac{\mu}{\rho c_p} \left[2 \left(\frac{\delta u_z}{\delta z} \right)^2 + 2 \left(\frac{\delta u_z}{\delta y} \right)^2 \right] \quad (2.49)$$

convection conduction viscous dissipation

It is usually adequate to neglect axial conduction and heat generation by viscous dissipation; in this case Eq.(2.49) reduces to

$$u_z \frac{dT}{dz} = \frac{k}{\rho c_p} \frac{d^2 T}{dy^2} \quad (2.50)$$

It is convenient to define a bulk temperature by the expression

$$T_b = \frac{1}{\Gamma} \int_0^b u_z T \, dy \quad (2.51)$$

The heat flux normal to the direction of flow is given by

$$q = -k \frac{\delta T}{\delta y} \quad (2.52)$$

and it follows from a heat balance that

$$\Gamma c_p \frac{dT}{dz} = q_w - q_i \quad (2.53)$$

where q_w is the heat flux from the wall to the film and q_i is the heat flux from the film (through the interface) to the gas phase.

Fully developed heat transfer can be defined as the condition in which

$$\frac{\delta T}{\delta z} \neq f(y) \quad (2.54)$$

thus it follows that

$$\frac{\delta T}{\delta z} = \frac{dT}{dz} = \frac{q_w - q_i}{\Gamma c_p} \quad (2.55)$$

and combining Eq.(2.55) and Eq.(2.50), one can obtain

$$\frac{d^2 T}{dy^2} = \frac{q_w - q_i}{\rho k \Gamma} u_z \quad (2.56)$$

Laminar flow solutions for heat transfer coefficients are obtained directly by integrating Eq.(2.56); details are given in the literature[24]. The results are summarised below:

(1) Falling film flows(zero interfacial shear)

(a) Heat transfer to liquid films only($q_i = 0$) in this case the heat transfer coefficient is defined by

$$h = \frac{q_w}{T_w - T_b} \quad (2.57)$$

and it can be shown that

$$h = \frac{280}{41} \frac{k}{b} = \frac{280}{41} \left(\frac{\rho^2 g k^3}{3\mu\Gamma} \right)^{1/3} \quad (2.58)$$

(b) Heat transfer with phase change(evaporation, $q_i = q_w$).

Here the local heat transfer coefficient is defined by

$$h = \frac{q_w}{T_w - T_i} \quad (2.59)$$

and the solution of the classical Nusselt one is

$$h = \frac{k}{b} = \left(\frac{\rho^2 g k^3}{3\mu\Gamma} \right)^{1/3} \quad (2.60)$$

(2) Essentially constant shear stress across the liquid film
(characteristics of high velocity annular flow)

(a) Heat transfer to films only ($q_i=0$). Here the heat transfer coefficient is defined as Eq.(2.57) and can be calculated as

$$h = \frac{q_w}{T_w - T_i} = \frac{15 k}{8 b} = \frac{15}{8} \left(\frac{\rho \tau_i k^2}{2\mu\Gamma} \right)^{1/2} \quad (2.61)$$

(b) Heat transfer with phase change (evaporation, $q_i=q_w$)
Here, the heat transfer coefficient is defined as in Eq.(2.59), and the laminar flow solution is as follows:

$$h = \frac{q_w}{T_w - T_i} = \frac{k}{b} = \left(\frac{\rho \tau_i k^2}{2\mu\Gamma} \right)^{1/2} \quad (2.62)$$

where τ_i is the interfacial shear stress at gas-liquid interface.

2.3.2 HEAT TRANSFER WITH TURBULENT FLOW

In the case of turbulent flow the action of the eddies enhances molecular conduction. Dukler[16] and Hewitt[23] used the following basic equations which outlines this problem in any position in the film.

$$\tau = (\mu + \epsilon \rho) \frac{du_z}{dy} \quad (2.63)$$

$$q = - (k + \epsilon_H \rho c_p) \frac{dT}{dy} \quad (2.64)$$

where ϵ is the eddy viscosity and ϵ_H the eddy thermal conductivity. Eq.(2.63) is concerned with mechanics of flow and the Eq.(2.64) deals with heat transfer. Its solution requires a knowledge of eddy thermal conductivity. The solution is based on the assumption that, in a convective field, momentum and energy are transported by similar mechanisms. In general, the values of

ϵ and ϵ_H depend on position, y , and velocity, u_z . The procedure generally used for predicting heat transfer in turbulent liquid film flows is to obtain values of ϵ from empirical correlations derived from single phase turbulent flows. Dukler and Hewitt used the following expressions of ϵ in their respective analyses of downward and upward annular film flow:

$$\epsilon = n^2 u_z y \left[1 - \exp\left(-\frac{\rho n^2 u_z y}{\mu}\right) \right] \quad (\text{Deissler, for } y^+ < 20) \quad (2.65)$$

$$\epsilon = \frac{K^* (du_z/dy)^3}{(d^2 u_z/dy^2)^2} \quad (\text{von Karman, for } y^+ > 20) \quad (2.66)$$

where y^+ is the "friction distance parameter" defined by Eq. (2.41). In the Deissler equation Eq. (2.65), n is a numerical constant and K^* in the von Karman equation Eq. (2.66) is a universal constant.

The rate equation for local heat transfer at any point in the tube has been expressed as [23]

$$\frac{q}{q_w} = \left(\frac{1}{Pr} + n^2 u^+ y^+ [1 - \exp(-n^2 u^+ y^+)] \right) \frac{dT^+}{dy^+} \quad (2.67)$$

For the case of evaporation ($q_i = q_w$), the following expression is obtained,

$$1 = \left(\frac{1}{Pr} + n^2 u^+ y^+ [1 - \exp(-n^2 u^+ y^+)] \right) \frac{dT^+}{dy^+} \quad (2.68)$$

where Pr is the Prandtl number, u^+ the dimensionless velocity defined by Eq. (2.40), and the dimensionless temperature T^+ is defined as

$$T^+ = \frac{c_p \rho u^*}{q_w} (T_w - T_i) \quad (2.69)$$

For the region $y^+ > 20$, k is small in comparison to the turbulent conduction term in Eq.(2.64). Neglecting the molecular conduction and combining Eqs.(2.64) and (2.66) in dimensionless form, the following expression is obtained

$$1 = K^* \frac{(du^+/dy^+)^2}{(d^2u^+/dy^{+2})^2} \frac{dT^+}{dy^+} \quad (2.70)$$

Eqs.(2.68) and (2.69) can be integrated across the liquid film to give a value of T_1^+ , which is defined in Eq.(2.69) with $T=T_1$, where T_1 is the interfacial temperature. Such integration can be carried out numerically, and a detailed description is given in the papers of Duckler[17] for downward flow and Hewitt [23] for upward flow.

Introducing Eq.(2.69) into Eq.(2.59), the heat transfer coefficient can be obtained as

$$h = \frac{c_p \rho u^+}{T_1^+} \quad (2.71)$$

It is convenient to express the result in terms of a liquid film Nusselt number, defined by

$$Nu = \frac{hb}{k} = \frac{Prb^+}{T_1^+} \quad (2.72)$$

where b^+ is the dimensionless film thickness defined by Eq. (2.42).

The value of b^+ can be determined by integrating expressions similar to Eqs.(2.68) and(2.70) for momentum transfer and determining the relationship between b^+ and W^+ . The dimensionless parameter W^+ is defined as

$$W^+ = \frac{\Gamma}{\mu} \quad (2.73)$$

The relationship between Nu and W^+ , and between b^+ and W^+ , are shown in Figure 2.4 for the case where the shear stress may be considered essentially constant across the film (i.e., Gravity effects are negligible).

The analytical expressions for the heat transfer have had variable success in predicting the actual coefficient, though coefficient data under strictly controlled conditions are rare. In general, the analysis tends to overpredict the heat transfer coefficient in evaporation but some what better results in condensation.

2.3.3 EMPIRICAL CORRELATION

2.3.3.1 LAMINAR FLOW

Experimental laminar flow heat transfer for liquid film are not plentiful. One of the earliest analyses of laminar heat transfer in falling film was done by Nusselt[33]. He derived the following equation for heat transfer to a liquid film flowing along a vertical surface.

$$h = \frac{\Gamma c_p}{L} \ln[1/(1 - \phi(s))] \quad (2.74)$$

where $\phi(s)$ is a function of the dimensionless group s , which can be represented by the following approximate equations:

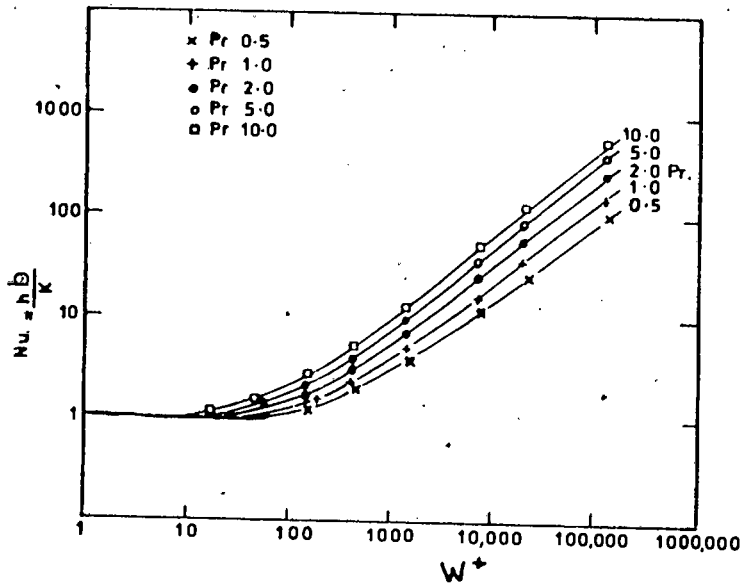
For $s < 0.05$

$$\phi(s) = 2.230 s^{0.656} \quad (2.75a)$$

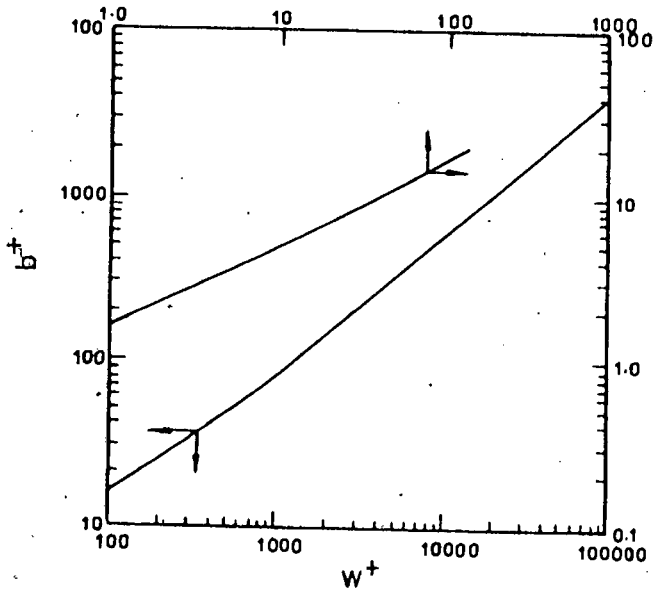
For $s > 0.05$

$$\phi(s) = 1 - 0.901e^{-0.656s} \quad (2.75b)$$

$$\text{where } s = \frac{k\mu L}{c_p \rho^2 g b^4}$$



(a)



(b)

Figure 2.4 Relationships between Nu and W^+ and between b^+ and W^+ from the analysis of Hewitt(1961).

The application of the classical Nusselt analysis to predict heat transfer to a falling liquid film was found grossly different from experimentally determined values[32]. Bays and McAdams[5] showed that the heat transfer coefficients for two petroleum oil films in laminar flow could be correlated by a modified form of this equation

$$\frac{hL}{c_p \Gamma} = 2.1 s^{2/3} (\mu/\mu_w)^{0.25} \quad (2.76)$$

Figure(2.5) shows the relevant data which were used for correlation of Eq.(2.76).

Adams et al[3] and Thompson[37] have presented a different empirical correlation for gravity flow of water over nearly horizontal pipes in the region of laminar flow. The correlation is expressed by the equation

$$h=65(\Gamma/D)^{1/3} \quad (2.77)$$

The correlation is shown in Figure 2.6. If the pipe diameter were very large or the mass flow rate were very small, a non-volatile liquid would leave the bottom of the tube at substantially the temperature of the wall of the pipe. For this limiting case, the definition of h , for negligible evaporation,

$$h = 4c_p \Gamma / \pi D \quad (2.78)$$

which is the equation of the asymptote AB of Figure 2.6.

2.3.3.2 TURBULENT FLOW

Several empirical correlations of heat transfer to turbulent water films on vertical and inclined surfaces have been reported. McAdams, Drew and Bays[30] correlated their results for turbulent flow of water film in a vertical tube by the equation

$$h=120\Gamma^{1/3} \quad (2.79)$$

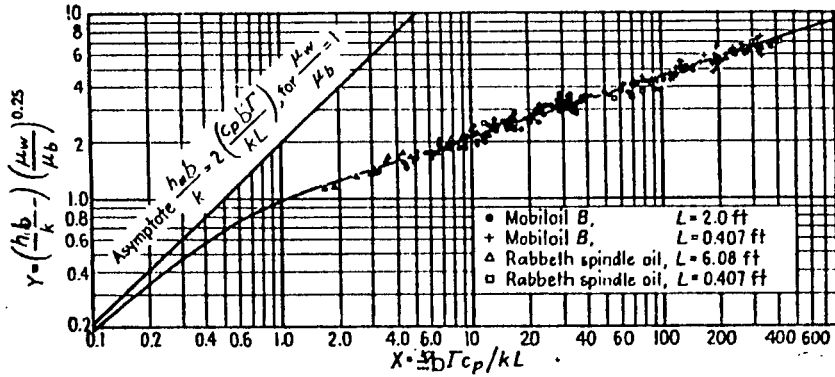


FIG. 2.5 Data for laminar flow in layer form down vertical tubes. [5]

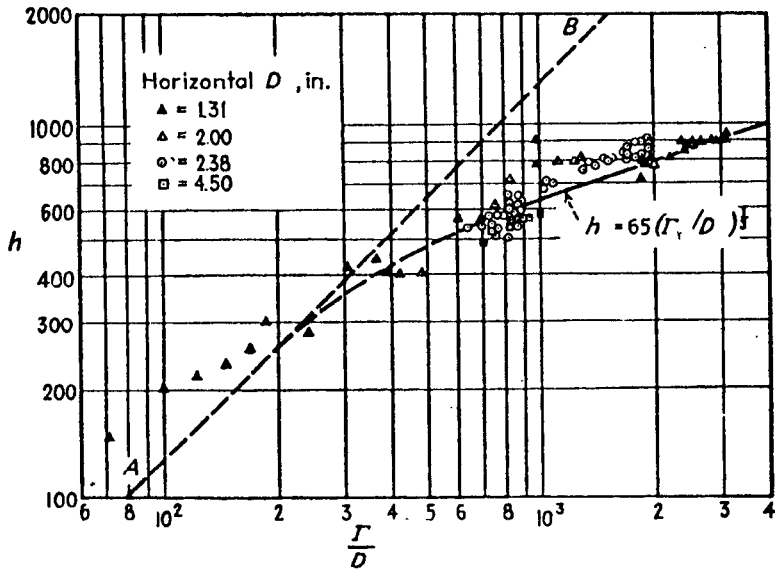


FIG. 2.6 Coefficients for gravity flow of water in layer form over nearly horizontal pipes. [37]

This correlation was obtained for length average heat transfer coefficients over a range of heat fluxes and water flow rates (Γ ranges from 600 to 15,000 lb of water per ft width of stream) in copper tubes heated externally by condensing steam.

Garwin and Kelly[20] measured the heat transfer coefficients to water films on vertical and inclined plates and correlated their results for a mean film temperature of 34° C by the equation

$$h = 87 (\sin \theta)^{0.2} \Gamma^{1/3} \quad (2.80)$$

where θ is the angle of the plate to the horizontal.

Brauer[8] formed the water film on vertical brass rod 4.5 ft long with an electrically heated section only 1/2 inch long at the lower end. The heat transfer coefficients were correlated by the equation

$$h = 886 \frac{k}{\mu} (4\Gamma/\mu)^{2/3} \quad (2.81)$$

Sexauer[36] correlated the heat transfer data for water falling down the outside of brass and iron pipe by the equation

$$h = \frac{a \Gamma^{0.5}}{L^{0.045}} (1 + 0.0142 T_m) \quad (2.82)$$

where the values of a 's were 14.5 and 10.5 for brass and iron pipes respectively; and T_m is the mean of the film and wall temperature in degree centigrade.

McAdams[31] recommends the use of the following equations, suggested by Drew for the calculation of values of the mean heat transfer coefficients in turbulent falling films.

$$h/\phi = 0.01 \text{Re}^{1/3} \text{Pr}^{1/3} \quad (2.83)$$

$$\text{where } \phi = \left(\frac{k^3 \rho^2 g}{\mu^2} \right)^{1/3}$$

This equation appears to be generalized, dimensionless form of the earlier dimensional Eq.(2.79) which correlated the results of McAdams, Drew and Bay[30] for turbulent falling film of water.

In 1963 from an experimental study using a relatively short tube, Ahmed and Kaparthy[2] obtained a correlation between a length-average heat transfer coefficients(incorporated in a modified Nusselt number, Nu^*) and Reynolds number over a wide range of Prandtl numbers. The relationship is

$$Nu^* = 0.00079 Re^{0.73} Pr^{0.4} (\mu/\mu_w)^{0.25} \quad (2.84)$$

In another experimental study Herbert and Sterns[22] obtained the following correlation for local heat transfer coefficients

$$h = 3.9 Re^{0.65} \quad (2.85)$$

This correlation was obtained for water flowing inside of a copper tube heated externally by electrical resistance heaters wound on the out side of the tube. The range of Reynolds number was 3,000-20,000 and water was in the non-boiling condition.

The local heat transfer coefficient for the evaporation of water falling in a film has been studied experimentally by Abou and Huyghe[1]. They established the following correlations using the mean square root method.

$$Nu = 0.0004 Re^{0.8} Pr^{0.7} \text{ for } Re_v < Re_{lim} \quad (2.86)$$

$$Nu = 0.0004 Re^{0.8} Pr^{0.7} (Re_v/Re_{lim}) \text{ for } Re_v > Re_{lim} \quad (2.87)$$

where,

Re_v = Reynolds number of the vapour in core

Re_{lim} = value of the limit of the Reynolds number which is equal to 25,000.

CHAPTER 3

OBJECTIVES OF THE WORK

The present work was undertaken to study the heat transfer characteristics of falling liquid films inside of a vertical tube. The objectives of this investigations were:

- (1) To measure the heat transfer coefficients of a falling liquid film inside a vertical tube.
- (2) To study the effect of film heat transfer coefficient with the change of flow rates and at different concentrations of urea in water.
- (3) To correlate the heat transfer coefficients in terms of relevant variables.

The thermal conductivity of urea solutions at different concentrations and temperatures were also determined.

CHAPTER 4

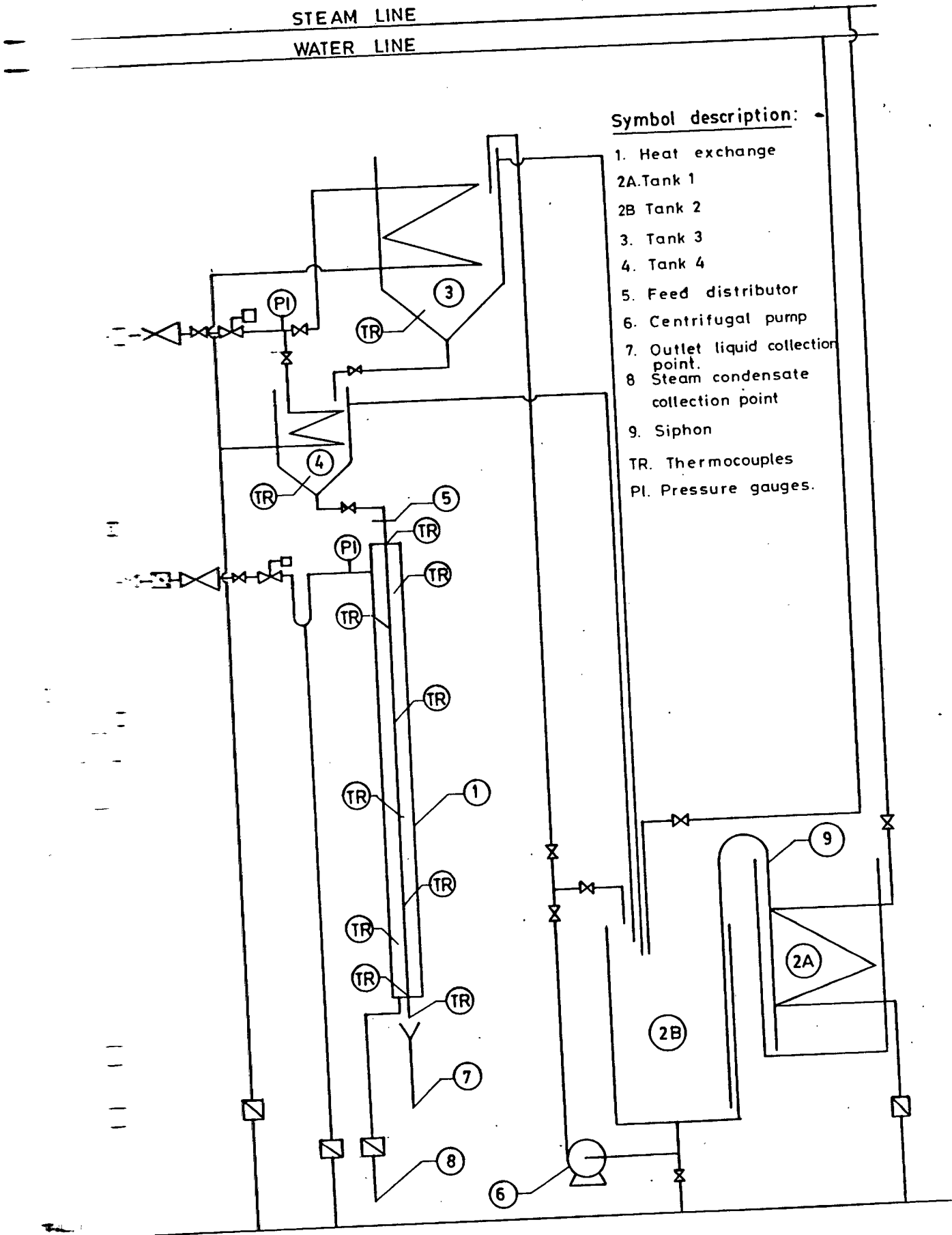
EXPERIMENTAL EQUIPMENT AND EXPERIMENTAL PROCEDUREINTRODUCTION

Heat transfer measurements were carried out using a double-pipe vertical heat exchanger which was designed, fabricated and tested for this purpose. The material of construction for heat exchanger, storage tanks, pipes and valves was stainless steel (type 304). Because stainless steel type 304 is one of the best materials of construction for urea solutions. Experimental fluid was urea solutions having a concentration range from 10 to 20% by weight. Thermal conductivity of the solutions was also measured.

EXPERIMENTAL EQUIPMENT

A schematic diagram of the experimental arrangement is shown in figure 4.1. A detailed description is given below:

- 1. A double pipe heat exchanger
- 2. Tank1, in which solution was prepared and stored.
- 3. Tank2, from which solution was transferred to the overhead tank.
- 4. Tank3, overhead tank.
- 5. Tank4, constant head tank.
- 6. Feed distributor.
- 7. Centrifugal pump, 2800 R.P.M., 1.5 H.P.
- 8. Outlet liquid collection point.
- 9. Steam condensate collection point.
- 10. Siphon
- 11. Thermocouples to temperature recorder
- 12. Pressure gauges



A Schematic Diagram of the Experimental Apparatus.

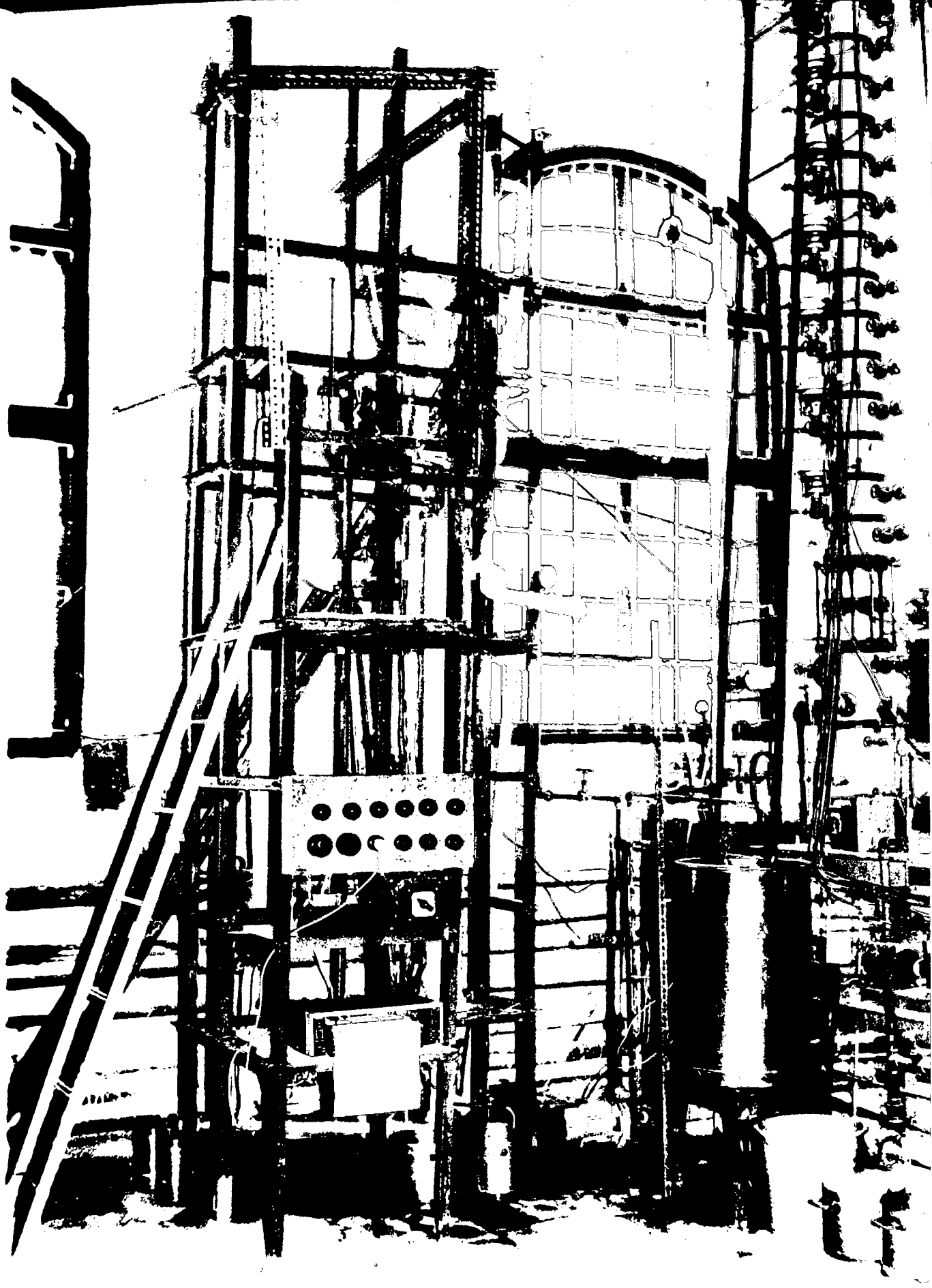


Figure 4.2 Photograph of the Experimental Apparatus

The general view of the set-up is shown in Figure 4.2.

The heat exchanger consisted of two thick-walled stainless steel concentric tubes. The inner tube was 3.24 cm. o.d. and 2.54 cm i.d. The working length of the tube was 2.0 m. The internal diameter of the jacket was 10.8 cm. The exchanger was lagged with asbestos rope and glass wool. The inner tube was separated from the outer tube with an O-ring made of asbestos rope which reduced heat conduction from the flange to the tube. A sectional view of the assembly of O-ring, inner tube and end flanges is shown in Figure 4.3.

Solutions were prepared and stored in tank1 which was fitted with a steam coil to permit heating. The capacity of the tank was 100 litre. The tank2 was equipped with a 2800 R.P.M. and 1.5 H.P. centrifugal pump to deliver the solution to the overhead storage tank (tank3). The overhead tank3 and the constant head tank4 were fitted with steam coil and lagged with magnesia for supplying the solution into the heat exchanger tube at a desired temperature. Tanks tank3 and tank4 were made from 1/16" thick stainless steel plate. tank2 was of PVC.

The feed distributor assembly was of stainless steel construction. Liquid entered into the distributor through the central hole and would come out through sixteen holes (1/16" diameter) towards the periphery and produce a film of liquid on the inside surface of the heat exchanger tube. The construction of the distributor assembly was developed based on of preliminary tests carried during the design stage of the set up. The detailed construction of the feed distributor assembly is shown in Figure 4.4.

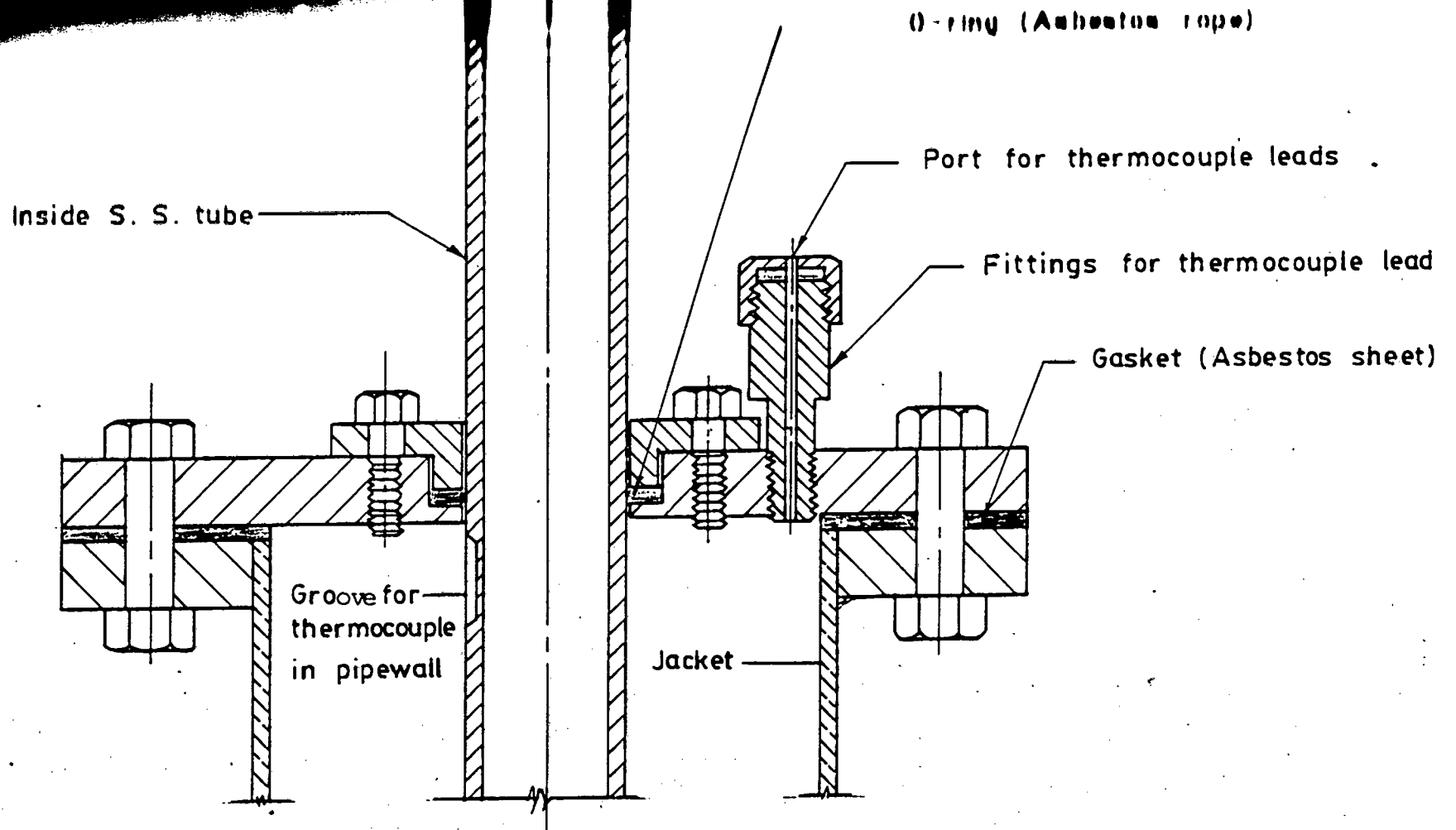


Fig. 4.3 A sectional view of the top section of the heat exchanger.

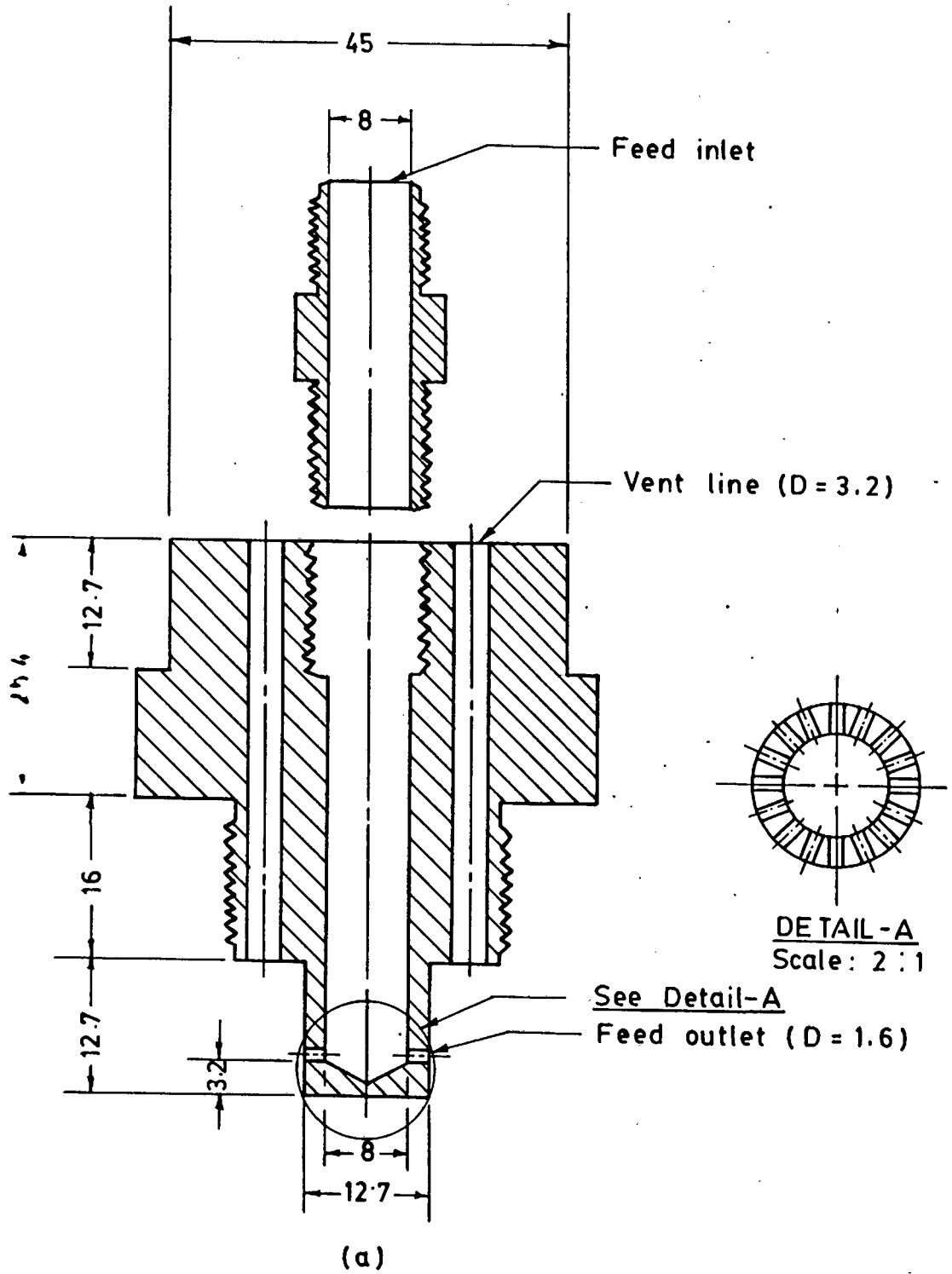


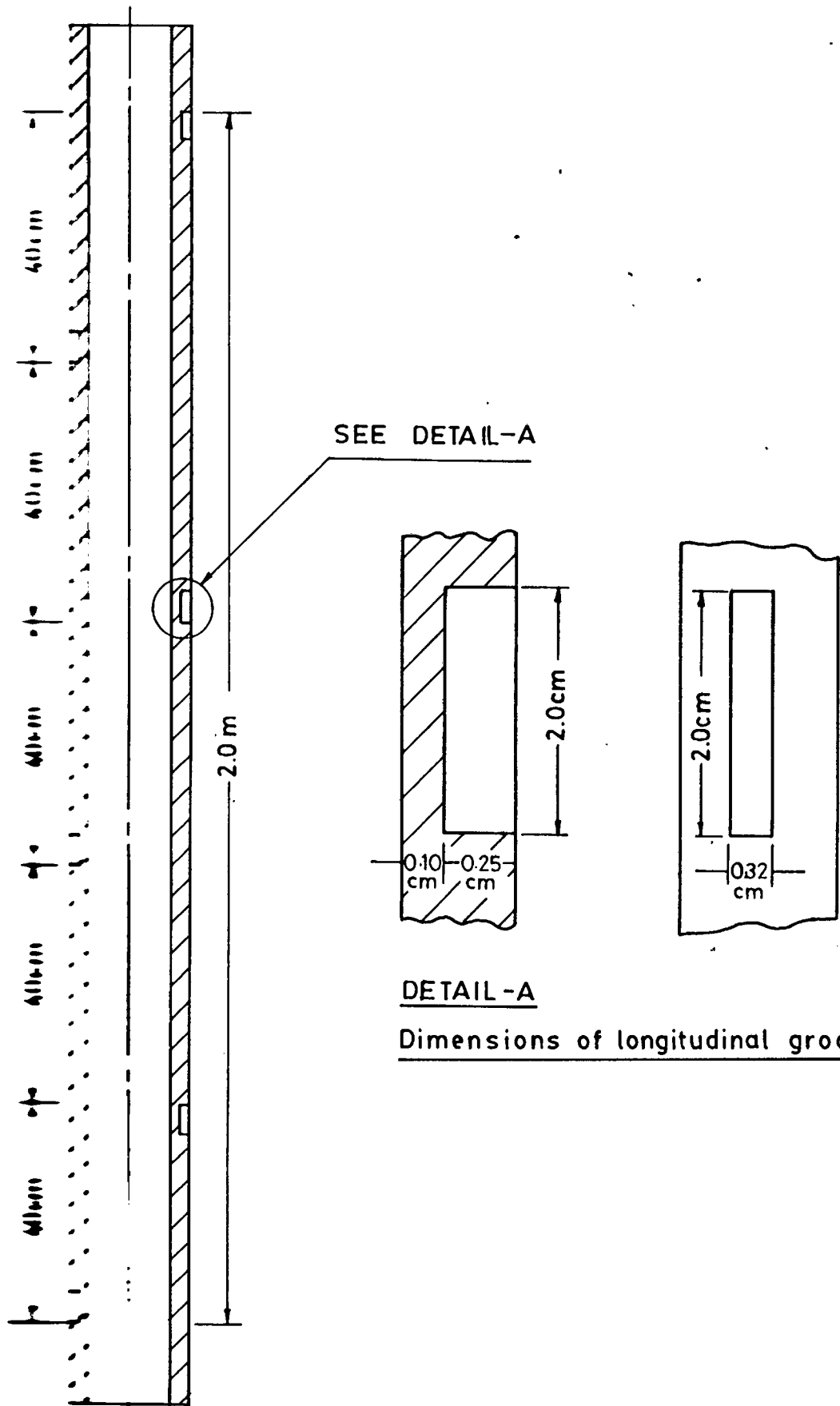
Figure 4.4 Construction of feed distributor.

The wall temperature of the inside tube was measured with thermocouples embedded into the outside wall of stainless steel tube and the leads were brought out of the exchanger section through ports in the flanges. The thermocouples on the outside wall were placed by milling longitudinal grooves 2.0 cm. x 0.32 cm. wide and 0.25 cm. deep in the wall at equal distances along the tube. Figure 4.5 shows the positions of thermocouples along the tube.

The inlet temperature of the fluid entering the heat exchanger was measured with a thermocouple placed in the constant temperature tank. The outlet temperature leaving the heat exchanger was measured with another thermocouple placed at the exit of the exchanger.

The temperature of the heating steam in the jacket of the heat exchanger was measured with two thermocouples located in the upper and lower section of the jacket. All the thermocouples were Chromel-Alumel type and were connected to a single-pen Philips recorder via a 12-point selector.

The steam used in the set-up was obtained by reducing the pressure of the available steam from 80-psig to 2-8 psig by means of pressure-reducing valves. Due care was taken to ensure that the steam entering into the exchanger was dry. The heat exchanger was provided with an air vent to bleed the entrapped air from the jacket. Pressure gauges were mounted on the wall of the exchanger to measure the steam pressure in the jacket.



DETAIL - A

Dimensions of longitudinal grooves.

Figure 4.5: Position of thermocouples along the tube.

4.3 EXPERIMENTAL PROCEDURE

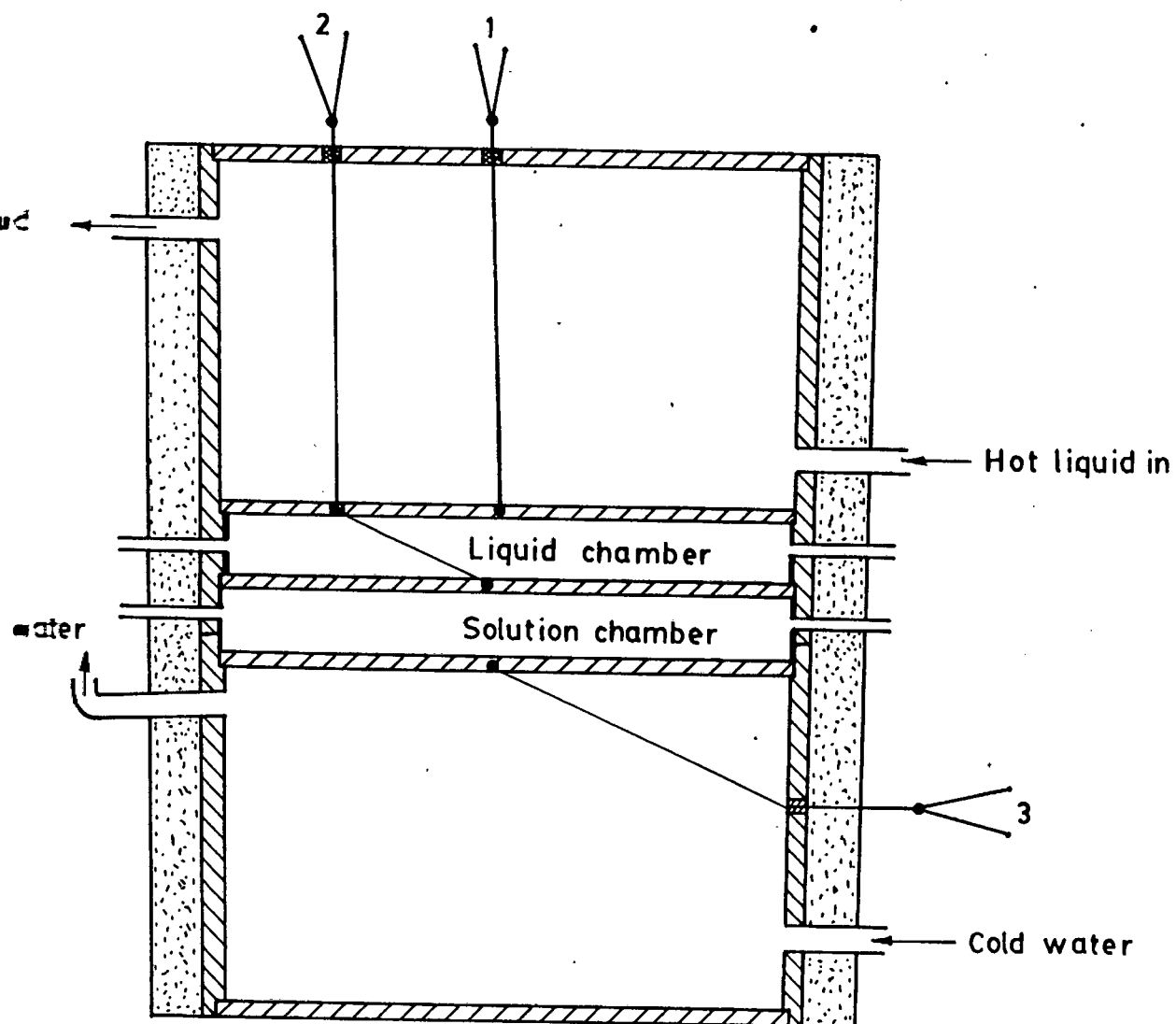
The experimental procedure was as follows:

- (1) A weighed amount of urea was added to the required amount of water in tank1 by stirring continuously. The mixture was then heated to a required temperature so that the solid urea completely dissolved in water.
- (2) The solution from tank1 was drawn to tank2 by means of a siphon(made of plastic tube).
- (3) The solution was drawn from tank2 by the centrifugal pump(2800 R.P.M., 1.5 H.P.) and pumped to the overhead storage tank, tank3.
- (4) The fluid was allowed to fall through the constant head tank, tank4, and distributing device in a film under gravity on the inside wall of the heat exchanger tube.
- (5) The flow rate of fluid was controlled by regulating a control valve and the flow rate was measured at the outlet by collecting the liquid in a bucket for a certain time interval.
- (6) The steam used for heating was made dry by separating moisture from it through separators, U-bend and traps before it entered into the exchangers and heaters. The pressure of the steam was reduced to 2-8 psig from 80 psig with a pressure reducing valve.

- (7) Venting of non-condensable gases from the heat exchanger jacket was regulated and was checked by comparing the saturated steam temperature and the thermocouples located in the upper section of the jacket and on the exchanger wall.
- (8) No heat transfer measurements were taken until the wall, inlet and outlet temperatures remained constant for ten to fifteen minutes. When the steady state was attained all the relevant temperatures, steam pressure and fluid flow rates were recorded. The measurements were taken over a period of five minutes.
- (9) In order to estimate the heat loss from the heat exchanger, it was run without fluid in the inside tube(blank) and the steam condensate in the jacket was collected. The amount of condensate collected was subtracted from that obtained with fluid flow inside tube for a heat balance based on steam condensate.
- (10) The heat exchanger tube was cleaned both before and after the measurements by passing hot water through it.

4.4 MEASUREMENT OF THERMAL CONDUCTIVITY

The construction and arrangement of the apparatus used to measure the thermal conductivity of urea solutions is schematically shown in Figure 4.6. It consisted of two chambers in which liquids could be maintained at constant but different temperatures separated by two other chambers into which the solution of unknown conductivity and a solution of known conductivity could






- 1, 2, 3 — Thermocouple leads
-  Insulation
-  Stainless steel
-  Thin araldite coating

Figure 4.6 Thermal-conductivity apparatus.

be placed. The chambers were externally insulated. Heat flowed through the contents of both chambers vertically. The horizontal element of each chamber were made of 1/16" stainless steel plate. Thermocouples were soldered to each plate. Each piece of plate was sealed to the vertical tube wall by means of araldite. A thin layer of araldite coating was also applied to the inside surface of the vertical wall of the conductivity chambers for minimizing the radial conduction from the wall to the liquid. The upper chamber was connected to a constant-temperature bath from which a constant hot water circulation was maintained. Through the lower chamber a circulation of cold water was maintained.

Experimental Procedure

First the experiment was carried out by pouring distilled water in both conductivity chambers. The thermocouple leads were connected to a single-pen Philips recorder through a 12-point selector. Cold water was circulated through the lower chamber and the upper chamber was connected to a constant hot water circulator and the device was allowed to attain constant temperatures i.e., steady state condition. It usually required three to five hours for reaching steady state temperature conditions. After steady state was attained, as indicated by temperature constancy, the temperatures were recorded. Distilled water from the lower conductivity chamber was then forced out by passing air through it. A solution of unknown conductivity was then introduced into this chamber and the experiment was carried out as described above.

CHAPTER 5

EXPERIMENTAL RESULTS

5.1 Proof of Experimental Procedure

The validity of the experimental procedure and the ability of the experimental apparatus to produce accurate and reproducible measurements were tested with water. Experiments were carried out both in laminar and turbulent regions. The experimental data along with calculated ones are presented in Tables 5.1a and 5.1b(Appendix-A). Heat balances based on the two streams were within $\pm 10\%$. The results obtained were consistent with the data available for similar systems in the literature[3,37]. The data were also reproducible which were evident from the experiments repeated.

5.2 Experimental Fluids and Their Physical and Thermal Properties

Experimental fluids included: water and solutions of urea in water. Concentrations of urea solutions ranged from 10 to 60% by weight. The characteristics of the experimental fluids are shown in Table 5.2. Fluid properties such as density, viscosity, and heat capacity were obtained from literature[11]. Correlations were used to calculate the fluid properties at different temperatures. The correlations used for viscosity calculation are shown in Table 5.3. The thermal conductivity of urea solutions were measured at two temperature levels and data for other temperatures were obtained by following the k-T data on water. The experimental data are shown in Table 5.4.

A total of 146 experimental measurements were carried out

using water and urea solutions with different concentrations given in table 5.2

Table 5.2 Experimental Fluids

Fluids	Temperature range °C	Density Kg/m ³	Heat capacity Kcal/Kg K	Thermal conductivity W/m °C	Viscosity Ns/m ² x10 ³
Water	55 - 65	986	1.00	0.649	0.5505
		981	1.00	0.660	0.4663
10% urea soln.	55 - 65	1012	0.93	0.715	0.5451
		1008	0.96	0.725	0.4800
20% urea soln.	60 - 70	1038	0.89	0.729	0.5640
		1034	0.92	0.741	0.4965
30% urea soln.	60 - 70	1066	0.83	0.753	0.6324
		1062	0.87	0.765	0.5536
40% urea soln.	65 - 75	1096	0.78	0.774	0.7199
		1092	0.82	0.786	0.6353
50% urea soln.	65 - 75	1125	0.74	0.777	0.8998
		1123	0.77	0.789	0.7976
60% urea soln.	70 - 75	1158	0.72	0.801	1.1085
		1156	0.73	0.807	1.0576

Table 5.3 Viscosity correlation

Conc. of solution (wt%)	viscosity correlation
0 (pure water)	$\mu = 1.37238 \times 10^{-3} \exp(-0.01661 \times T)$
10%	$\mu = 1.09730 \times 10^{-3} \exp(-0.01272 \times T)$
20%	$\mu = 1.21126 \times 10^{-3} \exp(-0.01274 \times T)$
30%	$\mu = 1.40636 \times 10^{-3} \exp(-0.01332 \times T)$
40%	$\mu = 1.62229 \times 10^{-3} \exp(-0.01250 \times T)$
50%	$\mu = 1.96925 \times 10^{-3} \exp(-0.01205 \times T)$
60%	$\mu = 2.13886 \times 10^{-3} \exp(-0.00939 \times T)$

Table 5.4 Thermal conductivity of urea solution

Urea solution % by weight	Avg. temperature of the fluid, °C	Thermal conductivity W/m °C
10	36.2	0.6890
	43.6	0.7028
20	36.5	0.7052
	43.7	0.7123
30	38.2	0.7322
	42.9	0.7357
40	38.4	0.7414
	44.5	0.7530
50	39.7	0.7494
	46.5	0.7582
60	47.0	0.7721

5.3 Experimental Results

A computer program was developed to analyse the experimental data. The program developed is shown in Appendix C. Heat balances were within $\pm 10\%$. While making calculations the following factors were considered.

- (a) Heat loss from the outside of the jacket was assumed to be constant over the entire length of the tube.
- (b) The wall temperature used was taken as the average of all the thermocouple readings in the tube wall.
- (c) Measured wall temperatures were corrected for the thermal resistance of the tube material.

- (d) The dirt film resistance was assumed to be negligible, because the tube was new and clean.
- (e) The value of the ΔT used in the calculation of heat transfer coefficient was taken as the difference between the average inside wall temperature and the mean bulk temperature of the fluid.
- (f) Physical properties such as μ , ρ , c_p and k were evaluated at mean bulk temperature of the fluid.

On the basis of these factors, the following two coefficients were calculated and shown in Tables 5.1a and 5.5a. h and J_i were calculated using the following definitions:

$$h = \frac{q}{\Delta T} \quad (5.1)$$

$$J_i = \frac{q}{\Delta T_{1m}} \quad (5.2)$$

The variables considered in the experimental investigations were: mass flow rate; inlet, outlet and wall temperatures; and concentrations of urea in water.

Eqs. (2.74) and (2.76) were used to predict the heat transfer coefficients for all 146 runs and the results are presented in Table 5.6 (Appendix-A). The agreement between the experimental and the predicted coefficients is poor.

In order to correlate the data, the dimensionless groups considered were Reynolds number, Prandtl number and Nusselt number by following the usual method of dimensional analysis. All these groups contained the relevant process variables, physical and thermal properties and important dimensions of the heat exchanger. The dimensionless groups were defined as:

$$\text{Reynolds number, } Re = \frac{4\Gamma}{\mu}$$

$$\text{Prandtl number, } Pr = \frac{C_p \mu}{k} ; \text{ and}$$

$$\text{Nusselt number, } Nu = \frac{hb}{k}$$

The calculated results such as h , U_1 , Γ , Re , Pr , Nu_{exp} , etc. are presented in Tables 5.1b and 5.5b(Appendix-A) for all experimental runs.

5.4 Analysis of Experimental Results

The influence of the different parameters on heat transfer are shown in Figures 5.1-5.6(Appendix-B). The plot of film heat transfer coefficients against mass flow rates per unit width of the tube for water and urea solutions are shown in Figures 5.1 and 5.3 respectively. The plot of film heat transfer coefficients against Reynolds number for water is shown in Figure 5.2 and that for urea solutions is shown in Figure 5.4.

All the experimental data were correlated using the dimensionless groups Re , Pr and Nu as outlined in section 5.3. The following correlation was established.

$$\text{Nu} = 4.3 \times 10^{-8} \text{Re}^{1.3} \text{Pr}^{1.71} \quad (5.3)$$

This relation correlates the data with a standard deviation of 3%. $\text{Nu}_{\text{expt}}/\text{Pr}^{1.71}$ against Re was plotted in Figure 5.5 to show that the Eq.(5.3) correlates the experimental data. Nu_{expt} against $\text{Nu}_{\text{calculated}}$ from Eq.(5.3) was plotted in Figure 5.6 for all 146 cases.

CHAPTER 6

DISCUSSION OF THE RESULTS

An experimental investigation was carried out so that the influence of liquid flow rate and liquid properties on the heat transfer coefficients of urea solutions in a falling film heat exchanger could be studied.

5. The h- Γ Plots for Water

The plot of film heat transfer coefficients, h , against mass flow rate per unit width of the tube, Γ , for water is shown in Figure 5.1. It is clear from this plot that heat transfer coefficients increase with Γ . The variation of heat transfer coefficients with Γ can be represented by the following equation[30].

$$h = \frac{\Gamma c_p}{L} \left[\frac{T_o - T_i}{T_p - (T_i + T_o)/2} \right] \quad (6.1)$$

This equation shows that the heat transfer coefficients depend on mass flow rate per unit width of the tube (Γ), heat capacity of the liquid (c_p) and inlet, outlet and average wall temperatures. The runs were carried out with water. Table 5.1 shows that outlet temperature of most of the runs are very close to the average wall temperature (T_p). The condition prevailing in the experiment is such that $T_p \approx T_o$. For this case, the Eq.(6.1) reduces to the simplified form given below:

$$h = \left(\frac{2c_p}{L} \right) \Gamma \quad (6.2)$$

The points which are seen above the line represented by the Eq. (6.2) indicated that the outlet temperatures for those runs were substantially higher than the average wall temperature.

5 : The h-Re Plots for Water

The plot of film heat transfer coefficients against Reynolds number for water is shown in Figure 5.2. This figure indicates that the heat transfer coefficients increase with Reynolds number. Following Eq.(6.2) and the conditions of the experiments as described in section 6.1, the equation h in terms of Re can be obtained as follows:

$$h = \left(\frac{C_p \mu}{2L} \right) Re \quad (6.3)$$

This equation indicates that heat transfer coefficient depends on heat capacity, viscosity and Reynolds number of the liquid film.

5 : The h-Γ Plots for Urea solutions

The plot of heat transfer coefficients against mass flow rate per unit width of the tube for urea solutions having concentration range from 10 to 60% by weight is shown in Figure 5.3. This figure indicates that heat transfer coefficient increases with Γ but decreases with the increase of concentration of the solution. The conditions of the outlet temperatures with urea solutions were the same as with water, i.e., the outlet temperature of most of the runs were very close to the temperature of the wall. In this case, as seen from Eq.(6.2), the heat transfer coefficients depend on heat capacity and mass flow rate per unit width of the tube. From Table 5.2 it is evident that heat

viscosity of the solution decreases with the increase of concentration.

The h-Re Plots for Urea solutions

The plots of film heat transfer coefficients, h , against Reynolds number for urea solutions are shown in Figure 5.4. From this figure it is observed that heat transfer coefficient increases with the Reynolds number. It is also observed that at any Re the heat transfer coefficient is independent of concentration of the solution upto 30%; however, beyond this concentration the heat transfer coefficient increases significantly.

Eq.(6.3) indicates that heat transfer coefficients depend on the product of heat capacity and the viscosity of the solution. The product of c_p and μ at mean bulk liquid temperature is essentially constant upto a concentration of 30% and increases thereafter, Table 6.1. The h-Re results of urea solutions thus show good agreement as evident from Figure 5.4.

Table 6.1 Product of c_p and μ

Urea soln. wt%	Mean bulk temp. °C	$c_p \times \mu$ W/m °C
10	60	2.036
20	65	1.996
30	65	2.107
40	70	2.268
50	70	2.697
60	75	3.234

Correlation of Heat Transfer Results

Measurement of heat transfer rates with water and urea solutions show that their heat transfer coefficients are different, Figures 5.1-5.4. The urea solutions show relatively low heat transfer coefficients on $h-F$ plots, Figure 5.3, but on $h-Re$ plots, Figure 5.4, the heat transfer coefficients does not change significantly at lower concentrations (upto 30 wt%) and increases at higher concentrations of the solution. For any useful heat transfer correlation, these systems are to be related with the relevant dimensionless groups.

The agreement between the experimental heat transfer coefficients and those predicted by Eqs. (2.74) and (2.76) for 146 runs is poor, Table 5.6 (Appendix-A). The theoretical equation of Nusselt, Eq. (2.74), shows that the heat transfer coefficients increase as Reynolds number decrease whereas the experimental results show the opposite. This discrepancy between the predicted and experimental result is probably due to the development of ripples in the liquid film. This has been supported by the other workers too [31,32]. At low Reynolds number, the experimental values are lower than those predicted by the empirical equation, Eq. (2.76), of Bays and McAdams [5]. At higher Reynolds number the data show limited agreement. It may be noted that the correlation, Eq. (2.76), was obtained for petroleum oils. Moreover, in the set-up used by Bays and McAdams, factors such as tube length and tube diameter, and, the method of liquid film distribution at the tube entry, were significantly different from those of the present work. The measured coefficients were

influenced to a considerable extent by the entrance effects in the short tubes used by those workers[5] and therefore, the empirical relation predicts higher coefficients.

The empirical correlation involving Re , Pr , and Nu in Eq. 5.3) correlates the heat transfer data for water and urea solutions. This correlation will calculate heat transfer rates reasonably well for urea solutions and similar solutions having the characteristics similar to those used in this work.

Nu and Re in the correlation are calculated for the liquid film. The characteristic length used is the film thickness. The film thickness does not appear in the expression of Re , but still remains in the expression of Nu . The film thickness has been determined using the Eq.(2.11) given in section 2.1.1 for the laminar flow of the film. Out of a total of 146 runs, 32 runs(22% of total) are in the turbulent range and wavy films may be encountered in this range. Actual measurement of velocity profile and film thickness in the turbulent range were not attempted and empirical correlations found in the literature do not give film thickness with a high degree of accuracy. Tables 5.1a , 5.1b, 5.5a and 5.5b (Appendix A) show that Re which fall in the turbulent range are not too high. Therefore, it is expected that the application of Eq.(2.11) to determine film thickness would not introduce significant error.

The thermal conductivity of the urea solutions were measured at two temperature levels and the data for the other temperatures were obtained by following the k-T data on water. The measurements

were not very accurate but a comparison with water was possible and an indicating variation of k with concentration was also obtained. Thermal conductivity thus measured were used to calculate the dimensionless groups such as Pr and Nu . From the plot of $Pr^{1.71}$ vs. Re , Figure 5.5, it is seen that the experimental data fits the correlation with a standard deviation of $\pm 9.0\%$.

The measured and predicted values of Nu with those predicted from Eq.(5.3) for all runs plotted in Figure 5.6 show that the correlation is satisfactory and the scattering of data is not significant.

The correlation obtained, Eq.(5.3), is applicable for similar systems in the following range:

$$Re = 660 - 4400$$

$$Pr = 2.4 - 4.1$$

CHAPTER 7

CONCLUSIONS

The following conclusions can be made on the basis of the study undertaken:

(1) Heat transfer coefficient increases with the increase of flow rate. On h - Γ plots, urea solutions show lower heat transfer coefficients with the increase of concentrations of urea solutions but on h - Re plots, it was observed that h is independent of concentration of the solution upto 30% and increases as the concentration increases thereafter.

(2) The heat transfer results are correlated using the following equation:

$$Nu = 4.3 \times 10^{-6} Re^{1.3} Pr^{1.71}$$

This equation can be used to calculate the heat transfer coefficients of a falling liquid film of water and aqueous solutions of urea with concentration ranging from 10 to 60% by weight and similar fluids in the following range:

$$Re = 660 - 4400$$

$$Pr = 2.4 - 4.1$$

(3) The thermal conductivities of urea solutions measured at two temperature levels show that they are greater than those of water.

CHAPTER 8

RECOMMENDATIONS FOR FUTURE WORK

- (1) More experimental investigations should be carried out with different types of solutions and liquids.
- (2) It is necessary to study the effect of tube dimensions such as diameter and length on the heat transfer coefficients.
- (3) The feed distributor should be redesigned to carry out heat transfer measurements with evaporation.
- (4) Heat transfer in the turbulent region would be useful.
- (5) A theoretical analysis of the problem may be useful.

NOMENCLATURE

- 1 Amplification of most unstable wave in travelling 10 cm.
- = film thickness
- 1 mean film thickness
- 1 tube diameter
- friction factor
- 1 acceleration of gravity
- film heat transfer coefficient
- ◀ constant, Eq.(2.35)
- ◀ universal constant, Eq.(2.66)
- ◀ thermal conductivity
- tube length
- ◀ mass flow rate
- constant in Eq.(2.65)
- = pressure
- = volumetric flow rate
- = heat flux
- = tube radius
- radial coordinates
- temperature
- T_i, T_o inlet and outlet temp. repectively
- T_b, T_m avg. bulk temp. equal to $(T_i + T_o)/2$
- T_w, T_p avg. wall temp. and avg. inside wall temp. respectively.
- velocity in z-direction
- mean velocity
- friction velocity, Eq.(2.43)
- film surface velocity
- gas stream velocity
- coordinate measured from wall across thickness of film
- = coordinates in the direction of flow

Dimensionless Groups

dimensionless film thickness, Eq.(2.42)

Froude number

Nusselt number

modified Nusselt number [2]

Prandtl number

Reynolds number

Reynolds number of gas stream

Reynolds number of vapour core

dimensionless quantity defined in Eqs.(2.75a) and (2.75b)

dimensionless velocity, Eq.(2.40)

dimensionless parameter defined in Eq.(2.73)

dimensionless distance, Eq.(2.41)

Greek Symbols

Liquid flow rate per unit width of the tube

change in quantity

angle of surface or tube, measured from horizontal

dynamic viscosity

density

ρ_{g0}

density of gas phase

surface tension

shear stress

interfacial shear stress

wall shear stress

pressure drop per unit length

function defined in Eqs.(2.75a) and (2.75b)

eddy viscosity

eddy thermal conductivity

quantity defined in Eq.(2.83)

Superscripts

- dimensionless quantity

Scripts

- $\bar{\cdot}$ average bulk
- \cdot inlet, interfacial
- \cdot outlet
- \bullet wall
- \cdot inside wall
- \cdot critical value of the quantity
- \cdot quasicritical value
- \cdot experimental quantity
- \cdot calculated quantity

Other symbols

- ∇^2 Laplacian operator
- $| \cdot |$ Absolute value of quantity f

REFERENCES

- Abou, P. and J. Huyghe, Experimental Study of Evaporator Heat Transfer in a Falling Film, Inst. Chem. Engrs. Symp. Ser. 38, Paper D5(1974).
- Ahmed, S. Y. and R. Kaparthi, Indian, J. Tech., 1,377(1963).
- Adams, F.W., G. Broughton and A.L. Conn, A Horizontal Film-Cooler(Film Coefficients of Heat Transmission), Ind. Eng. Chem., 28, 537(1936).
- Barba, D. and A. Giona, The Pressure Loss in a Falling Film Evaporator, British Chem. Eng., 15, 1436(1970).
- Bays, G. S. and W. H. McAdams, Heat Transfer Coefficients in Falling-Film Heaters, Ind. Eng. Chem., 29, 1240(1937).
- Binne, A. M., Experiments on the Onset of Wave Formation on a Film of Water Flowing Down a Vertical Plane, Fluid Mech. J., 2, 1(1957).
- Bird, R. B., W. E. Stewart and E. N. Lightfoot, Transport Phenomena, Jhon Wiley and Sons, Inc, New York(1960).
- Brauer, H., Forschungsh, Stromung und Wärmeübergang bei Flüssigfilmen, VDI(Ver. Deut. Ingr.), No. 457(1956).
- Brauer, H., Chem. Ing. Tech., 32, 719(1960).
- Brooke-Benjamin, T., Fluid. Mech. J., 2, 554(1957).
- Chao, G. T., Urea Its Properties and Manufacture, Chao's Institute, West Covina, Calif.
- Copper, C. M., T. B. Drew, and W. H. McAdams, Isothermal Flow in Liquid Layers, Ind. Eng. Chem., 26, 428(1934).
- Davies, J. T. and A. M. Shawki, Heat Transfer from Turbulent Falling Films of Water and Non-Newtonian Solutions on Smooth and Ridge Plates, Chem. Eng. Sci., 29, 1801(1974).
- Deissler, R. G., Analysis of Turbulent Heat Transfer, Mass Transfer and Friction in Smooth Tubes at high Prandtl and Schmidt numbers, NACA Rep.1210(1955).

5. Dukler, A. E. and O. P. Bergelin, Characteristics of Flow in Falling Liquid Films, Chem. Eng. Progr., 48, 557(1952).
6. Dukler, A. E., Fluid Mechanics and Heat Transfer in Falling Film Systems, Chem. Eng. Progr., Symp. Ser., No. 30, 56 1(1960).
7. Feind, K., Stromungsuntersuchungen bei Gegenstrom von Flüssigfilmen und Gas in lotrechten Röhren, VDI(Ver. Deut. Ingr.)-Forschungsh, 481(1960).
8. Friedman, S. J. and C. O. Miller, Liquid Films in the Viscous Flow Region, Ind. Eng. Chem., 33, 385(1941).
9. Fulford, G. D., The Flow of Liquid in Thin Films, Advances in Chemical Engineering, edited by Drew, T. B. et al, vol. 5, Academic Press, New York(1964).
10. Garwin, L. and E. W. Kelly, Ind. Chem. Eng., 47, 392(1955).
11. Grimley, S. S., Liquid Flow Conditions in Packed Towers, Trans. Inst. Chem. Engrs., 23, 228(1945).
12. Herbert, L. S. and U. J. Sterns, An Experimental Investigation of Heat Transfer to Water in Film Flow, Part 1: Non-Boiling Runs with and without induced swirl, Canadian J., Chem. Eng., 46, 401(1968).
13. Hewitt, G. F., Analysis of Annular Two Phase Flow: Application of the Dukler Analysis to Vertical Upward Flow in a Tube, AERE-R3680(1961).
14. Hewitt, G. F. and N. S. Hall-Taylor, Annular Two Phase Flow, Pergamon Press, New York(1970).
15. Jackson, M. L., Liquid Films Flow in Viscous Flow, A.I.Ch.J., 1, 235(1955).
16. Kapitza, P. L., Zh. Exp. Teg. Fis, 18, 3(1948).
17. Kirkbride, C. G., Heat Transfer by condensing Vapor on Vertical Tubes, Ind. Eng. Chem., 26, 425(1934).
18. Levich, V. G., Zh. Fiz. Khim., 22, 721(1948).

1. Levich, V. G., Fiziko-Khimicheskaya Hidrodinamika, 2nd ed. Gostizdatgiz, Moscow, 1959; English Translation Published as Physico-Chemical Hydrodynamics, Prentice-Hall, Englewood Cliffs, New Jersey (1962).
2. McAdams, W. H., T. B. Drew and G. S. Bays, Heat Transmission in Falling Water-Films, Trans. A.S.M.E., 62, 627 (1940).
3. McAdams, W. H., Heat Transmission, 3rd ed., p. 245, McGraw-Hill (1954).
4. Norman, W. S. and V. McIntyre, Heat Transfer to a Liquid Film on a Vertical Surface, Trans. Inst. Chem. Eng., 38, 111 (1960).
5. Nusselt, W., Die Abhängigkeit der Wärmeübergangszahl von der Rohrlänge, VDI (Ver. Deut. Ingr.) Z, 54, 1154 (1910).
6. Nusselt, W., Die Oberflächenkondensation des Wasserdampfes, VDI (Ver. Deut. Ingr.) Z, 60, 541 (1916).
7. Semenov, P. A., Zh. Tekhn. Fiz., 14, 427 (1944).
8. Sexauer, T., Forsch. Ing. Wes., 10, 286 (1938).
9. Thompson, A. K. G., Heat Transmission in Film-Type Collars, Trans. Soc. Chem. Ind., 56, 380T (1937).
10. von Karman, T., Analogy between Friction and Heat Transfer, Trans. A.S.M.E., 61, 705 (1939).
11. Yih, C. S., Proc. 2nd. U. S. Congr. Appl. Mech., 623 (1954).
12. Young, E. and J. R. Sinek, Evaporation 5: Heat Transfer in Falling-Film Long-tube Vertical Evaporators, Chem. Eng. Progr., 74 (1962).

APPENDIX A
TABLES (page 60-80)

Heat Transfer Data for Water

Run	Mass Flow Rate Kg/hr	Fluid Temp. Ti To	Avg. wall Temp. Tw C	Steam Temp. Ts C	Qi W	Qj W	% Heat Balance	Heat Flux W/m ²	Corrected Wall Temp. Tp C	Avg. Temp. Diff. ΔT C	Overall Log mean Temp. diff. ΔT _{lm} C
1	42.7	25.6 88.2	90.5	105.0	3111.	3069.	-1.36	17942.	88.8	31.9	40.3
2	44.0	25.6 87.8	90.2	103.1	3183.	3128.	-1.74	18322.	88.5	31.8	38.3
3	64.4	25.6 86.2	89.7	105.0	4539.	4690.	3.21	26796.	87.2	31.3	42.1
4	67.7	25.6 86.0	88.8	105.0	4757.	4933.	3.56	28132.	86.2	30.4	42.2
5	98.6	25.6 85.8	88.7	103.1	6904.	6996.	1.31	40354.	85.0	29.3	40.1
6	102.8	25.6 85.5	88.6	103.1	7160.	7356.	2.66	42145.	84.7	29.2	40.4
7	106.6	25.6 85.2	88.0	105.0	7389.	7642.	3.31	43636.	84.0	28.6	42.9
8	114.3	25.6 84.6	86.6	103.1	7843.	7950.	1.35	45853.	82.4	27.3	41.2
9	117.7	25.6 83.4	85.9	103.1	7912.	8053.	1.75	46352.	81.6	27.1	42.2
10	132.1	25.6 82.5	83.9	103.1	8744.	8879.	1.52	51162.	79.2	25.1	42.9
11	50.8	37.8 95.2	95.4	105.0	3391.	3546.	4.36	20141.	93.5	27.0	29.8
12	82.1	37.8 92.7	92.8	105.0	5242.	5528.	5.17	31268.	89.9	24.7	32.3
13	96.4	36.6 92.3	91.8	106.0	6244.	6602.	5.42	37295.	88.4	23.9	34.3
14	60.5	36.6 93.0	91.7	104.0	3966.	4343.	8.69	24124.	89.5	24.7	31.1
15	88.9	41.3 92.1	89.3	104.0	5252.	5488.	4.29	31182.	86.4	19.7	30.6
16	126.8	40.8 89.2	88.2	104.0	7139.	7426.	3.87	42287.	84.3	19.3	33.3

Heat Transfer Data for Water (continued)

Run	Mass Flow Rate Kg/hr	Fluid Temp. C Ti To	Avg. wall Temp. Tw C	Steam Temp. Ts C	Qi W	Qj W	% Heat Balance	Heat Flux W/m ²	Corrected Wall Temp. Tp C	Avg. Temp. Diff. ΔT C	Overall Log mean Temp. diff. ΔT _{lm} C
17	136.4	38.1 87.2	87.6	104.0	7789.	7747.	-.54	45103.	83.4	20.8	35.9
18	115.7	42.0 92.7	89.5	104.0	6820.	6764.	-.83	39438.	85.9	18.5	29.8
19	76.7	43.7 93.1	91.3	104.0	4404.	4536.	2.91	25956.	88.9	20.5	28.9
20	41.9	35.0 94.0	93.6	106.0	2876.	2932.	1.93	16863.	92.0	27.5	33.2
21	54.1	38.4 93.7	91.8	106.0	3477.	3558.	2.27	20426.	89.9	23.9	32.5
22	63.0	40.0 92.7	91.2	105.0	3864.	4148.	6.85	23263.	89.1	22.7	31.7
23	59.2	37.4 93.0	91.6	105.0	3828.	4106.	6.78	23034.	89.5	24.3	32.2
24	170.2	30.5 81.5	83.8	103.0	10094.	9721.	-3.84	57529.	78.5	22.5	42.0
25	152.5	32.3 82.4	84.2	103.0	8888.	8827.	-.70	51431.	79.5	22.1	40.6
26	141.1	33.6 84.5	85.0	103.0	8351.	8232.	-1.44	48144.	80.6	21.5	38.5
27	130.8	34.2 87.8	87.8	103.0	8155.	8113.	-.52	47228.	83.4	22.4	35.5
28	50.1	36.0 89.1	92.4	105.0	3095.	3189.	2.94	18245.	90.7	28.2	36.2
29	66.0	34.2 88.4	90.5	105.0	4157.	4344.	4.31	24683.	88.2	26.9	37.4
30	83.5	35.6 87.2	87.7	103.0	5009.	5323.	5.91	29996.	84.9	23.5	35.6
31	101.3	36.0 86.8	88.4	103.0	5987.	6228.	3.88	35463.	85.1	23.7	35.8
32	115.5	36.6 86.6	87.8	103.0	6718.	6721.	.04	39016.	84.2	22.6	35.8

Table 5.1b
Calculated Results for Water

Mass Flow rate kg/hr	Peripheral Mass Flow Rate Kg/hr.m	h W/m ² C	U ₁ W/m ² C	Re	Pr	Nu (expt)	Nu (calc)	Nu -- Pr ^{1.71}
42.7	535.5	561.8	445.3	1115.	3.4	.25	.32	.031
44.0	551.5	576.2	478.1	1144.	3.4	.26	.34	.032
44.4	807.3	855.5	637.2	1653.	3.5	.44	.55	.052
47.7	848.8	925.5	666.3	1735.	3.5	.49	.59	.058
48.6	1235.9	1378.7	1005.5	2523.	3.5	.82	.96	.097
48.8	1288.2	1445.5	1043.3	2623.	3.5	.88	1.01	.104
48.6	1336.0	1527.4	1017.1	2713.	3.5	.94	1.07	.110
44.3	1432.6	1681.8	1113.6	2895.	3.5	1.06	1.17	.123
47.7	1475.3	1709.2	1098.7	2952.	3.5	1.09	1.22	.125
48.1	1656.1	2036.3	1191.7	3289.	3.6	1.35	1.42	.153
48.8	636.7	745.0	675.8	1555.	2.9	.34	.38	.055
48.1	1029.0	1268.0	967.4	2461.	3.0	.68	.71	.106
48.4	1208.1	1560.2	1086.7	2852.	3.0	.88	.88	.134
48.5	757.8	977.9	775.6	1799.	3.0	.47	.48	.072
48.9	1114.3	1581.3	1020.4	2730.	2.9	.86	.78	.139
48.8	1589.6	2191.5	1268.7	3786.	3.0	1.35	1.25	.209
48.4	1709.5	2169.9	1255.9	3916.	3.1	1.39	1.40	.201
48.7	1449.7	2130.8	1324.6	3591.	2.9	1.26	1.09	.208
48.7	960.8	1266.1	899.0	2422.	2.8	.65	.64	.111
48.9	525.3	612.4	508.3	1241.	3.0	.26	.30	.040
44.1	677.7	856.1	629.6	1643.	2.9	.40	.41	.064
48.0	790.2	1024.9	735.1	1925.	2.9	.50	.50	.080
48.2	741.9	949.1	716.4	1773.	3.0	.45	.47	.070
48.2	2133.0	2558.1	1371.6	4376.	3.5	1.83	1.95	.218
48.5	1911.9	2327.0	1266.3	4011.	3.4	1.59	1.68	.197
48.1	1768.1	2238.8	1250.9	3815.	3.3	1.48	1.50	.192
48.8	1639.6	2104.8	1330.8	3655.	3.2	1.34	1.34	.185
48.1	628.2	647.9	504.5	1437.	3.1	.30	.38	.043
48.9	826.6	917.0	660.7	1852.	3.2	.46	.55	.064
48.5	1046.1	1274.9	843.5	2347.	3.2	.70	.75	.097
48.3	1270.1	1494.9	991.4	2850.	3.2	.87	.96	.121
48.5	1448.0	1726.7	1091.5	3260.	3.2	1.05	1.14	.147

Heat Transfer Data for Urea solutions

Run	Mass Flow Kg/hr	Fluid Temp.C ----- Ti To	Avg. wall Temp. Tw C	Steam Temp. Ts C	Qi W	Qj W	% Heat Balance	Heat Flux W/m ²	Corrected Wall Temp. Tp C	Avg. Temp. Temp. ΔT C	Overall Log mean Temp.diff. ΔTlm C
10% urea solution											
33	38.1	19.5 90.3	94.3	105.0	2980.	3027.	1.55	17442.	92.7	37.8	40.2
34	53.8	19.5 89.1	92.6	105.0	4133.	3952.	-4.59	23474.	90.4	36.1	41.4
35	64.0	19.5 86.4	89.7	105.0	4727.	4865.	2.83	27849.	87.1	34.2	43.9
36	40.8	29.3 95.5	95.7	105.0	2986.	3077.	2.97	17603.	94.1	31.7	31.9
37	50.3	29.3 94.8	95.5	105.0	3644.	3839.	5.08	21723.	93.5	31.4	32.7
38	65.3	29.3 93.0	94.4	105.0	4597.	4916.	6.49	27619.	91.9	30.7	34.6
39	62.6	29.3 92.1	93.4	105.0	4343.	4604.	5.67	25976.	91.0	30.3	35.5
40	61.2	33.0 95.2	93.0	105.0	4208.	4237.	.69	24519.	90.7	26.6	31.2
41	55.8	36.6 92.5	93.5	105.0	3446.	3314.	-3.98	19625.	91.7	27.1	32.9
42	63.3	39.1 95.2	94.0	105.0	3922.	3904.	-.45	22722.	91.9	24.8	29.4
43	74.2	41.5 94.0	93.0	105.0	4302.	4270.	-.74	24886.	90.7	23.0	29.9
44	80.3	43.3 94.0	93.6	105.0	4497.	4506.	.20	26140.	91.2	22.5	29.4
45	73.5	45.1 94.6	93.4	105.0	4019.	4086.	1.65	23530.	91.2	21.4	28.3
46	71.2	47.6 96.0	93.6	105.0	3808.	3844.	.92	22215.	91.6	19.8	26.1
47	64.0	48.8 97.2	95.6	105.0	3420.	3226.	-6.01	19296.	93.8	20.8	24.5
48	39.7	48.8 97.5	95.2	105.0	2138.	2270.	5.80	12796.	94.0	20.9	24.2

Heat Transfer Data for Urea solutions(continued)

Run	Mass Flow Rate Kg/hr	Fluid Temp. Ti To	Avg. wall Temp. Tw C	Steam Temp. Ts C	Qi W	Qj W	% Heat Balance	Heat Flux W/m ²	Corrected Wall Temp. Tp C	Avg. Temp. Diff. ΔT C	Overall Log mean Temp. diff. ΔT _{lm} C
20% urea solution											
49	35.4	23.8 96.4	97.0	108.0	2689.	2790.	3.64	15906.	95.5	35.4	36.6
50	58.5	23.8 95.2	96.0	107.0	4373.	4391.	.41	25444.	93.7	34.2	36.6
51	71.4	25.6 94.0	94.8	107.0	5115.	5051.	-1.25	29515.	92.1	32.3	37.3
52	57.8	29.3 96.3	95.3	107.0	4056.	4076.	.50	23609.	93.1	30.3	33.8
53	38.5	33.3 99.4	97.1	108.0	2661.	2732.	2.60	15659.	95.7	29.3	30.6
54	69.1	36.6 96.4	97.0	107.0	4324.	4167.	-3.76	24652.	94.7	28.2	31.6
55	85.0	39.1 91.5	92.7	107.0	4665.	4393.	-6.19	26296.	90.3	25.0	35.5
56	32.7	40.7 100.0	96.0	107.0	2027.	2059.	1.55	11863.	94.9	24.6	26.4
57	29.9	42.8 101.3	97.5	108.0	1833.	1894.	3.19	10819.	96.5	24.5	25.7
58	74.2	39.1 95.2	93.7	107.0	4355.	4405.	1.14	25432.	91.4	24.2	32.1
59	136.1	41.5 89.1	91.1	106.0	6780.	6744.	-.53	39262.	87.5	22.2	35.5
60	68.0	46.4 96.4	95.4	106.0	3561.	3565.	.12	20688.	93.5	22.1	27.4
61	102.5	51.2 95.2	94.3	106.0	4721.	4729.	.17	27437.	91.8	18.6	27.1
62	71.4	33.6 94.0	96.8	106.0	4517.	4692.	3.74	26735.	94.3	30.5	33.6
63	98.7	33.6 90.3	94.0	106.0	5855.	5896.	.69	34116.	90.9	28.9	37.1
64	65.3	33.6 94.0	94.8	106.0	4129.	4194.	1.55	24166.	92.6	28.8	33.6

Heat Transfer Data for Urea solutions(continued)

Run	Mass Flow Rate Kg/hr	Fluid Temp. Ti To	Avg. wall Temp. Tw C	Steam Temp. Ts C	Qi W	Qj W	% Heat Balance	Heat Flux W/m ²	Corrected Wall Temp. Tp C	Avg. Temp. ΔT C	Overall Log mean Temp.diff. ΔT _{lm} C
20% urea solution											
65	82.3	35.8 92.7	94.1	106.0	4903.	4938.	.70	28570.	91.5	27.2	34.2
66	93.2	35.4 91.5	92.8	106.0	5473.	5485.	.21	31815.	89.9	26.4	35.4
30% urea solution											
67	30.4	38.8 99.2	99.1	108.0	1815.	1866.	2.77	10686.	98.1	29.1	29.3
68	39.9	38.8 98.6	97.2	108.0	2360.	2340.	-.86	13643.	95.9	27.2	30.0
69	43.2	37.8 97.6	96.4	107.5	2555.	2561.	.24	14855.	95.0	27.3	30.6
70	44.9	35.4 95.2	95.9	107.5	2655.	2684.	1.08	15498.	94.5	29.2	33.8
71	62.6	36.0 90.3	93.8	105.0	3360.	3264.	-2.95	19230.	92.0	28.9	35.1
72	84.4	36.6 89.1	91.6	105.0	4379.	4403.	.56	25495.	89.2	26.4	36.0
73	112.3	37.2 88.5	91.1	105.0	5693.	5571.	-2.19	32704.	88.1	25.2	36.3
74	98.0	38.4 89.1	91.7	105.0	4910.	4812.	-2.05	28227.	89.1	25.3	35.4
75	78.2	40.3 91.0	93.0	105.0	3922.	3905.	-.43	22722.	90.9	25.3	33.1
76	68.7	41.5 94.6	94.4	105.0	3607.	3622.	.40	20988.	92.5	24.4	29.3
77	43.5	34.6 96.4	98.3	107.0	2660.	2707.	1.71	15581.	96.9	31.4	32.2

Heat Transfer Data for Urea solutions(continued)

Run	Mass Flow Rate Kg/hr	Fluid Temp.C Ti To	Avg. wall Temp. Tw C	Steam Temp. Ts C	Qi W	Qj W	% Heat Balance	Heat Flux W/m ²	Corrected Wall Temp. Tp C	Avg. Temp. Diff. ΔT C	Overall Log mean Temp.diff. ΔT _{lm} C
30% urea solution											
78	59.9	34.6 95.2	97.4	107.0	3587.	3665.	2.14	21054.	95.5	30.6	33.4
79	78.9	34.2 94.0	96.4	107.0	4666.	4708.	.90	27215.	93.9	29.8	34.7
80	91.6	34.2 91.5	94.1	107.0	5190.	5188.	-.05	30129.	91.3	28.5	37.0
81	111.1	35.4 90.3	93.4	107.0	6031.	6257.	3.61	35675.	90.1	27.3	37.7
82	129.3	37.8 90.3	93.2	107.0	6709.	6625.	-1.26	38714.	89.6	25.6	36.9
83	44.2	47.6 97.6	97.6	106.0	2186.	2258.	3.18	12901.	96.4	23.8	25.8
84	61.9	48.8 96.4	97.1	106.0	2913.	2912.	-.06	16912.	95.5	22.9	26.7
85	75.5	49.4 95.8	95.3	106.0	3464.	3475.	.31	20146.	93.4	20.8	27.1
86	96.2	49.4 92.7	94.0	106.0	4116.	4097.	-.48	23843.	91.8	20.8	29.9
40% urea solution											
87	49.0	17.7 91.5	95.3	106.2	3364.	3609.	6.79	20242.	93.4	38.8	41.1
88	63.3	18.3 87.7	93.9	106.2	4086.	4257.	4.03	24221.	91.7	38.7	44.5
89	82.3	18.9 89.1	92.6	105.0	5377.	5385.	.15	31246.	89.7	35.7	41.6
90	102.7	20.8 87.8	89.5	105.0	6404.	6154.	-4.07	36461.	86.1	31.8	42.2

Table 6.6a

Heat Transfer Data for Urea solutions(continued)

Run	Mass Flow Rate Kg/hr	Fluid Temp. Ti To C	Avg. wall Temp. Tw C	Steam Temp. Ts C	Qi W	Qj W	% Heat Balance	Heat Flux W/m ²	Corrected Wall Temp. Tp C	Avg. Temp. Diff. ΔT C	Overall Log mean Temp. diff. ΔT _{lm} C
40% urea solution											
91	115.7	27.0 86.6	89.8	105.0	6414.	6435.	.32	37303.	86.4	29.6	41.3
92	133.5	30.5 86.6	89.7	105.0	6970.	6999.	.42	40556.	86.0	27.4	40.1
93	85.3	32.3 92.7	92.0	105.0	4792.	4851.	1.22	27997.	89.4	26.9	34.0
94	43.5	48.8 97.6	98.3	106.2	1977.	2085.	5.18	11794.	97.2	24.0	25.7
95	59.2	48.8 94.5	96.1	106.2	2517.	2650.	5.03	15001.	94.7	23.1	28.7
96	73.5	47.6 92.7	93.5	106.2	3083.	3383.	8.86	18774.	91.8	21.6	30.7
97	84.4	47.6 92.2	93.2	106.2	3501.	3704.	5.48	20917.	91.3	21.4	31.2
98	93.2	48.8 92.2	92.6	105.0	3764.	3895.	3.36	22235.	90.6	20.1	29.3
99	106.8	49.4 91.5	92.5	105.0	4184.	4318.	3.10	24684.	90.2	19.8	29.7
100	122.0	50.0 90.9	91.8	105.0	4643.	4702.	1.26	27132.	89.3	18.8	30.0
101	140.3	51.2 89.1	91.1	105.0	4949.	5108.	3.12	29198.	88.4	18.3	31.1
102	120.8	51.2 92.1	91.8	105.0	4597.	4868.	5.57	27477.	89.3	17.6	28.6
103	36.3	34.2 98.8	99.3	108.6	2181.	2420.	9.86	13357.	98.1	31.6	31.9
104	48.3	34.2 95.8	94.2	107.4	2769.	2870.	3.54	16371.	92.7	27.7	33.4
105	59.9	34.2 92.7	94.6	107.4	3259.	3323.	1.94	19110.	92.8	29.4	36.4
106	68.0	34.8 92.7	93.9	107.4	3665.	3696.	.82	21370.	91.9	28.2	36.3

Heat Transfer Data for Urea solutions(continued)

Run	Mass Flow Rate Kg/hr	Fluid Temp. Ti To	Avg. wall Temp. Tw C	Steam Temp. Ts C	Qi W	Qj W	% Heat Balance	Heat Flux W/m ²	Corrected Wall Temp. Tp C	Avg. Temp. ΔT C	Overall Log mean Temp.diff. ΔTlm C
50% urea solution											
107	43.5	28.1 94.0	95.6	106.0	2536.	2540.	.14	14738.	94.2	33.2	35.2
108	59.9	28.1 91.5	94.9	105.0	3355.	3187.	-5.26	18995.	93.1	33.3	36.4
109	72.1	28.1 90.3	92.1	105.0	3965.	3809.	-4.10	22570.	90.0	30.8	37.6
110	86.4	29.3 89.7	92.5	105.0	4613.	4657.	.93	26912.	90.0	30.5	37.8
111	101.7	30.5 88.5	92.1	105.0	5216.	4934.	-5.72	29466.	89.4	29.9	38.5
112	113.6	34.0 87.8	92.1	105.0	5403.	5199.	-3.93	30781.	89.3	28.4	37.9
113	119.1	37.8 89.1	91.5	105.0	5399.	5384.	-.28	31305.	88.6	25.2	35.6
114	44.5	26.8 97.7	99.3	109.5	2791.	2700.	-3.39	15942.	97.8	35.6	36.4
115	59.9	26.8 95.5	98.0	109.5	3636.	3517.	-3.38	20766.	96.1	34.9	38.7
116	72.1	26.8 93.3	93.2	108.6	4239.	4305.	1.52	24805.	90.9	30.9	39.7
117	83.0	28.7 94.0	95.5	108.6	4791.	4839.	1.00	27959.	92.9	31.6	38.4
118	95.3	31.7 92.7	94.9	108.6	5136.	5149.	.25	29858.	92.1	29.9	38.7
119	108.2	36.6 92.7	94.8	108.6	5364.	5319.	-.85	31017.	91.9	27.3	37.1
120	119.1	39.5 92.1	93.4	108.6	5536.	5458.	-1.42	31918.	90.5	24.7	36.7
121	138.6	45.1 92.7	93.8	108.6	5832.	5850.	.30	33915.	90.7	21.8	34.4
122	125.9	48.6 94.0	94.6	108.6	5051.	5036.	-.30	29285.	91.9	20.6	32.1

Heat Transfer Data for Urea solutions (continued)

Run	Mass Flow Rate Kg/hr	Fluid Temp. Ti To	Avg. wall Temp. Tw C	Steam Temp. Ts C	Qi W	Qj W	% Heat Balance	Heat Flux W/m ²	Corrected Wall Temp. Tp C	Avg. Temp. Diff. ΔT C	Overall Log mean Temp. diff. ΔT _{lm} C
50% urea solution											
123	118.4	51.7 95.2	95.0	106.0	4552.	4558.	.13	26448.	92.6	19.1	26.9
124	107.5	54.0 95.2	94.7	106.0	3915.	3891.	-.62	22661.	92.6	18.0	26.2
125	93.9	53.0 95.8	94.6	106.0	3552.	3496.	-1.60	20462.	92.7	18.3	26.0
126	78.9	53.0 96.4	95.4	106.0	3028.	3045.	.57	17630.	93.8	19.1	25.4
60% urea solution											
127	65.3	55.0 97.6	99.1	109.0	2362.	2445.	3.38	13957.	97.8	21.5	27.4
128	78.9	55.0 96.4	97.8	109.0	2774.	2858.	2.94	16351.	96.3	20.6	28.4
129	89.8	54.0 95.8	97.0	109.0	3187.	3148.	-1.25	18392.	95.3	20.4	29.3
130	99.8	54.0 95.2	96.4	109.0	3490.	3373.	-3.49	19925.	94.6	20.0	29.8
131	108.2	54.0 94.6	95.6	109.0	3729.	3740.	.31	21685.	93.6	19.3	30.3
132	115.7	54.0 94.0	95.6	108.0	3928.	3860.	-1.77	22610.	93.5	19.5	29.6
133	127.6	55.0 94.0	95.4	108.0	4225.	4220.	-.11	24518.	93.1	18.6	29.3
134	134.4	56.0 93.3	94.9	108.0	4256.	4333.	1.77	24936.	92.6	18.0	29.5
135	115.7	56.5 95.2	95.4	108.0	3800.	3658.	-3.90	21652.	93.4	17.6	27.8

Table 3.5a
Heat Transfer Data for Urea solutions(continued)

Run	Mass Flow Rate Kg/hr	Fluid Temp.C Ti To	Avg. wall Temp. Tw C	Steam Temp. Ts C	Qi W	Qj W	% Heat Balance	Heat Flux W/m ²	Corrected Wall Temp. Tp C	Avg. Temp. Temp.	Overall Log mean Diff. Temp.diff. ΔT C	Overall Log mean Temp.diff. ΔTlm C
60% urea solution												
136	106.1	57.0 95.8	96.4	107.5	3496.	3432.	-1.86	20116.	94.5	18.1	26.5	
137	97.3	57.0 96.4	97.0	107.5	3255.	3264.	.28	18924.	95.3	18.6	26.0	
138	89.8	57.2 97.6	97.8	107.5	3080.	2982.	-3.29	17602.	96.2	18.8	24.9	
139	78.9	57.0 98.2	98.0	107.5	2761.	2701.	-2.21	15856.	96.5	18.9	24.4	
140	66.4	56.5 98.8	98.1	108.0	2383.	2363.	-.84	13780.	96.8	19.2	24.6	
141	73.9	56.5 97.6	97.2	108.0	2580.	2504.	-3.03	14760.	95.8	18.8	25.7	
142	76.9	56.5 97.0	97.5	108.0	2644.	2645.	.04	15353.	96.1	19.3	26.2	
143	79.6	56.5 97.0	97.5	108.0	2737.	2757.	.73	15952.	96.0	19.3	26.2	
144	83.0	55.0 96.4	97.1	108.0	2918.	2898.	-.68	16884.	95.5	19.8	27.2	
145	88.5	55.0 96.0	96.2	108.0	3079.	3010.	-2.27	17679.	94.6	19.1	27.6	
146	92.5	55.0 95.7	95.2	108.0	3197.	3233.	1.12	18670.	93.5	18.1	27.9	

Table 5.5b
Calculated Results for Urea solution

Mass Flow rate of Kg/hr	Peripheral Mass Flow Rate Kg/hr.m	h W/m ² C	U _i W/m ² C	Re	Pr	Nu (expt)	Nu (calc)	Nu -- Pr ^{1.71}
<u>urea solution</u>								
38.1	477.5	461.7	433.9	972.	3.0	.18	.22	.027
53.8	673.7	649.8	567.5	1360.	3.0	.28	.34	.042
64.0	801.6	815.0	635.2	1591.	3.1	.38	.43	.055
40.8	511.7	555.9	552.0	1145.	2.7	.21	.23	.038
50.3	631.0	691.0	665.0	1406.	2.8	.29	.30	.051
65.3	818.7	899.8	798.8	1804.	2.8	.41	.43	.071
62.6	784.5	857.4	732.2	1719.	2.8	.38	.40	.065
61.2	767.5	920.7	786.4	1756.	2.7	.40	.38	.074
55.8	699.3	723.3	596.9	1609.	2.7	.31	.34	.058
63.3	793.1	918.1	772.1	1886.	2.6	.40	.39	.079
74.2	929.5	1084.4	831.3	2227.	2.6	.50	.48	.100
80.3	1006.3	1160.1	889.3	2439.	2.5	.55	.53	.113
73.5	921.0	1100.9	832.5	2267.	2.5	.50	.47	.105
71.2	892.6	1125.1	850.7	2252.	2.4	.50	.45	.110
64.0	801.6	927.0	787.5	2053.	2.4	.40	.39	.090
39.7	498.0	613.3	529.3	1278.	2.4	.22	.21	.050
<u>urea solution</u>								
35.4	443.4	449.0	434.4	874.	2.9	.17	.18	.028
58.5	733.4	745.2	696.2	1435.	2.9	.33	.34	.053
71.4	895.4	914.7	791.8	1759.	2.9	.43	.44	.070
57.8	724.8	778.8	698.8	1479.	2.8	.33	.33	.057
38.5	482.1	534.5	512.3	1029.	2.7	.20	.19	.037
69.1	865.8	873.6	780.8	1852.	2.7	.39	.41	.073
35.1	1065.9	1053.2	741.5	2246.	2.7	.51	.54	.093
32.7	409.3	483.3	449.9	920.	2.5	.17	.15	.035
29.9	375.2	442.6	421.0	862.	2.5	.15	.13	.032
74.2	929.5	1051.0	793.5	2005.	2.6	.48	.44	.091
36.1	1705.5	1770.7	1105.1	3593.	2.7	1.00	.99	.182

Table 5.5b
Calculated Results for Urea solution(continued)

Mass Flow rate mf Kg/hr	Peripheral Mass Flow Rate Kg/hr.m	h W/m2 C	Ui W/m2 C	Re	Pr	Nu (expt)	Nu (calc)	Nu -- Pr ^{1.71}
<u>urea solution</u>								
68.0	852.8	936.7	755.7	1942.	2.5	.41	.39	.086
102.5	1284.8	1477.9	1013.1	2994.	2.5	.74	.66	.160
71.4	895.4	875.8	795.8	1851.	2.8	.40	.43	.071
98.7	1236.5	1180.7	920.0	2496.	2.8	.61	.66	.104
65.3	818.7	840.2	719.3	1692.	2.8	.37	.38	.065
82.3	1031.8	1050.1	835.6	2145.	2.7	.50	.52	.089
93.2	1168.3	1204.7	898.0	2404.	2.8	.61	.61	.107
<u>urea solution</u>								
30.4	380.9	367.2	365.0	754.	2.6	.12	.12	.023
39.9	500.3	501.0	455.6	987.	2.6	.18	.18	.034
43.2	541.8	543.7	485.0	1054.	2.7	.20	.20	.037
44.9	562.8	531.5	458.5	1061.	2.8	.21	.21	.037
62.6	784.5	666.1	547.8	1437.	2.8	.29	.33	.048
84.4	1057.4	966.0	708.8	1929.	2.9	.47	.48	.078
112.3	1407.1	1296.4	901.2	2567.	2.9	.69	.70	.115
98.0	1228.0	1113.9	797.7	2267.	2.8	.56	.58	.095
78.2	980.7	900.0	686.2	1857.	2.8	.42	.43	.075
68.7	861.3	859.9	715.3	1684.	2.7	.38	.36	.071
43.5	545.8	496.9	484.6	1031.	2.8	.19	.20	.034
59.9	750.4	689.2	630.5	1407.	2.8	.29	.31	.051
78.9	989.2	913.8	784.3	1835.	2.8	.43	.44	.074
91.6	1148.4	1058.5	813.6	2095.	2.9	.52	.54	.086
111.1	1392.8	1309.1	946.2	2541.	2.9	.69	.69	.115
129.3	1620.3	1513.9	1048.6	3003.	2.8	.84	.84	.144
44.2	554.3	542.0	500.5	1151.	2.5	.20	.20	.041
61.9	776.0	737.4	634.3	1612.	2.5	.31	.31	.064
75.5	946.6	966.9	744.2	1966.	2.5	.43	.40	.089
96.2	1205.2	1149.3	797.7	2452.	2.6	.56	.55	.112

Table 5.5b

Calculated Results for Urea solution(continued)

Mass Flow rate mf kg/hr	Peripheral Mass Flow Rate Kg/hr.m	h W/m ² C	U _i W/m ² C	Re	Pr	Nu (expt)	Nu (calc)	Nu -- Pr ^{1.71}
<u>urea solution</u>								
49.0	614.0	521.4	492.5	832.	3.5	.22	.23	.026
63.3	793.1	626.6	544.1	1053.	3.6	.29	.33	.032
82.3	1031.8	875.0	752.1	1387.	3.5	.44	.46	.050
102.7	1287.7	1145.5	864.6	1738.	3.5	.62	.61	.071
115.7	1449.7	1262.3	904.3	2019.	3.4	.71	.70	.086
133.5	1673.7	1480.0	1011.3	2382.	3.3	.86	.83	.109
85.3	1068.8	1040.4	823.8	1598.	3.2	.51	.46	.070
43.5	545.8	491.3	458.9	933.	2.8	.19	.18	.033
59.2	741.9	650.5	522.2	1244.	2.8	.27	.27	.045
73.5	921.0	868.7	611.3	1515.	2.9	.39	.36	.063
84.4	1057.4	979.0	671.7	1734.	2.9	.47	.43	.076
93.2	1168.3	1109.3	758.2	1931.	2.9	.55	.49	.090
106.8	1338.8	1248.7	830.2	2211.	2.9	.64	.59	.104
122.0	1529.3	1439.9	903.2	2526.	2.9	.77	.70	.126
140.3	1759.0	1599.7	939.4	2894.	2.9	.90	.84	.146
120.8	1513.9	1560.2	959.7	2538.	2.8	.83	.69	.139
36.3	454.8	423.2	419.2	715.	3.0	.15	.15	.022
48.3	605.5	591.4	489.7	934.	3.1	.24	.22	.035
59.9	750.4	650.5	524.6	1136.	3.2	.28	.29	.039
68.0	852.8	758.6	589.7	1295.	3.1	.35	.34	.050
<u>urea solution</u>								
43.5	545.8	444.2	418.5	642.	3.8	.19	.19	.019
59.9	750.4	569.8	521.4	870.	3.9	.27	.29	.026
72.1	903.9	732.6	600.6	1040.	3.9	.36	.37	.035
86.4	1083.0	882.1	712.6	1251.	3.9	.47	.47	.046
101.7	1275.2	986.3	766.1	1473.	3.9	.55	.58	.053
113.6	1424.1	1085.6	811.4	1673.	3.8	.62	.67	.062
119.1	1492.3	1244.4	879.8	1808.	3.7	.72	.70	.076
44.5	558.3	448.2	438.0	667.	3.8	.19	.20	.020

Table 5.5b

Calculated Results for Urea solution(continued)

Mass Flow rate mf Kg/hr	Peripheral Mass Flow Rate Kg/hr.m	h W/m2 C	Ui W/m2 C	Re	Pr	Nu (expt)	Nu (calc)	Nu -- Pr ^{1.71}
<u>urea solution</u>								
59.9	750.4	594.6	537.0	884.	3.8	.28	.29	.028
72.1	903.9	804.0	625.5	1051.	3.9	.40	.37	.039
83.0	1040.4	885.8	728.0	1229.	3.8	.46	.44	.046
95.3	1193.9	997.3	771.8	1425.	3.8	.54	.53	.055
108.2	1355.9	1136.9	835.3	1667.	3.7	.63	.62	.068
119.1	1492.3	1294.9	869.3	1860.	3.6	.74	.69	.082
138.6	1737.4	1558.1	986.9	2248.	3.5	.93	.83	.110
125.9	1577.6	1422.1	912.0	2101.	3.4	.81	.72	.101
118.4	1483.8	1384.3	982.2	2028.	3.3	.77	.66	.100
107.5	1347.4	1258.6	864.8	1867.	3.3	.67	.58	.089
93.9	1176.8	1117.7	788.1	1627.	3.3	.57	.49	.075
78.9	989.2	924.6	694.3	1372.	3.3	.45	.39	.060
<u>urea solution</u>								
65.3	818.7	649.0	509.7	870.	4.0	.31	.30	.029
78.9	989.2	794.3	575.0	1046.	4.0	.40	.39	.037
89.8	1125.7	901.7	628.1	1181.	4.0	.48	.46	.044
99.8	1250.7	998.4	668.9	1309.	4.1	.55	.53	.050
108.2	1355.9	1123.9	716.0	1415.	4.1	.63	.59	.057
115.7	1449.7	1158.9	763.3	1508.	4.1	.67	.65	.061
127.6	1599.2	1315.8	837.2	1672.	4.1	.78	.73	.071
134.4	1684.5	1389.5	844.8	1763.	4.1	.84	.78	.077
115.7	1449.7	1233.8	779.1	1535.	4.0	.71	.64	.066
106.1	1330.3	1108.9	758.4	1416.	4.0	.62	.57	.059
97.3	1219.4	1020.2	727.9	1301.	4.0	.55	.51	.052
89.8	1125.7	937.7	708.4	1209.	4.0	.49	.46	.047
78.9	989.2	837.5	651.4	1064.	3.9	.42	.39	.040
66.4	831.7	718.7	561.3	895.	3.9	.34	.31	.033

Table 5.5b
 Calculated Results for Urea solution(continued)

Mass Flow rate mf Kg/hr	Peripheral Mass Flow Rate Kg/hr.m	h W/m ² C	U _i W/m ² C	Re	Pr	Nu (expt)	Nu (calc)	Nu -- Pr ^{1.71}
<u>urea solution</u>								
73.9	926.7	785.8	574.7	992.	4.0	.39	.36	.037
76.9	963.6	794.3	585.4	1029.	4.0	.40	.37	.038
79.6	997.7	827.6	608.2	1065.	4.0	.42	.39	.040
83.0	1040.4	851.1	619.8	1100.	4.0	.44	.42	.041
88.4	1108.6	927.3	640.7	1170.	4.0	.49	.45	.045
92.5	1159.8	1030.2	670.3	1222.	4.0	.55	.48	.051

Coefficient of correlation= .985979

% Standard Deviation= 9.029

Table 5.6
Comparison of Experimental Coefficients
with those from Eqs. (2.74) and (2.76)

Run	Re	h from Eq. (2.74)	h from Eq. (2.76)	h in the present work
<u>water</u>				
1	1115.	4217.	1336.	562.
2	1144.	4173.	1338.	576.
3	1653.	3677.	1389.	856.
4	1735.	3617.	1391.	925.
5	2523.	3216.	1443.	1379.
6	2623.	3173.	1448.	1446.
7	2713.	3136.	1450.	1527.
8	2895.	3066.	1451.	1682.
9	2952.	3030.	1452.	1709.
10	3289.	2921.	1456.	2036.
11	1555.	4204.	1382.	745.
12	2461.	3585.	1437.	1268.
13	2852.	3396.	1454.	1560.
14	1799.	3938.	1387.	978.
15	2730.	3525.	1428.	1581.
16	3786.	3136.	1473.	2192.
17	3916.	3031.	1481.	2170.
18	3591.	3264.	1466.	2131.
19	2422.	3726.	1418.	1266.
20	1241.	4424.	1346.	612.
21	1643.	4110.	1371.	856.
22	1925.	3919.	1390.	1025.
23	1773.	3974.	1383.	949.
24	4376.	2747.	1492.	2558.
25	4011.	2853.	1479.	2327.
26	3815.	2944.	1472.	2239.
27	3655.	3041.	1476.	2105.
28	1437.	4131.	1367.	648.
29	1852.	3758.	1395.	917.
30	2347.	3492.	1412.	1275.
31	2850.	3290.	1444.	1495.
32	3260.	3165.	1460.	1727.

Table 5.6

Comparison of Experimental Coefficients
with those from Eqs.(2.74) and (2.76)(continued)

Run	Re	h from Eq.(2.74)	h from Eq.(2.76)	h in the present work
<u>10% urea solution</u>				
33	972.	4863.	1374.	462.
34	1360.	4338.	1418.	650.
35	1591.	4079.	1431.	815.
36	1145.	4907.	1387.	556.
37	1406.	4577.	1418.	691.
38	1804.	4194.	1452.	900.
39	1719.	4243.	1441.	857.
40	1756.	4335.	1435.	921.
41	1609.	4475.	1424.	723.
42	1886.	4345.	1444.	918.
43	2227.	4141.	1464.	1084.
44	2439.	4053.	1478.	1160.
45	2267.	4189.	1464.	1101.
46	2252.	4266.	1459.	1125.
47	2053.	4438.	1452.	927.
48	1278.	5180.	1378.	613.
<u>20% urea solution</u>				
49	874.	5112.	1353.	449.
50	1435.	4330.	1422.	745.
51	1759.	4067.	1446.	915.
52	1479.	4407.	1416.	779.
53	1029.	5108.	1363.	534.
54	1852.	4228.	1450.	874.
55	2246.	3938.	1463.	1053.
56	920.	5481.	1333.	483.
57	862.	5680.	1326.	443.
58	2005.	4145.	1445.	1051.
59	3593.	3407.	1528.	1771.
60	1942.	4337.	1439.	937.
61	2994.	3839.	1497.	1478.
62	1851.	4136.	1455.	876.

Table 5.6
 Comparison of Experimental Coefficients
 with those from Eqs.(2.74) and (2.76)(continued)

Run	Re	h from Eq.(2.74)	h from Eq.(2.76)	h in the present work
<u>20% urea solution</u>				
63	2496.	3707.	1492.	1181.
64	1692.	4256.	1432.	840.
65	2145.	3961.	1464.	1050.
66	2404.	3797.	1477.	1205.
<u>30% urea solution</u>				
67	754.	5656.	1329.	367.
68	987.	5165.	1360.	501.
69	1054.	5010.	1369.	544.
70	1061.	4896.	1373.	531.
71	1437.	4355.	1414.	666.
72	1929.	3954.	1448.	966.
73	2567.	3616.	1489.	1296.
74	2267.	3787.	1471.	1114.
75	1857.	4100.	1443.	900.
76	1684.	4319.	1428.	860.
77	1031.	4950.	1379.	497.
78	1407.	4452.	1423.	689.
79	1835.	4061.	1460.	914.
80	2095.	3852.	1472.	1059.
81	2541.	3627.	1498.	1309.
82	3003.	3481.	1520.	1514.
83	1151.	5082.	1376.	542.
84	1612.	4556.	1424.	737.
85	1966.	4275.	1446.	967.
86	2452.	3933.	1478.	1149.
<u>40% urea solution</u>				
87	832.	4462.	1334.	521.
88	1053.	4081.	1365.	627.
89	1387.	3767.	1396.	875.
90	1738.	3518.	1415.	1146.

Table 5.6

Comparison of Experimental Coefficients
with those from Eqs.(2.74) and (2.76)(continued)

Run	Re	h from Eq.(2.74)	h from Eq.(2.76)	h in the present work
<u>40% urea solution</u>				
91	2019.	3426.	1433.	1262.
92	2382.	3302.	1454.	1480.
93	1598.	3858.	1396.	1040.
94	933.	5009.	1323.	491.
95	1244.	4504.	1359.	651.
96	1515.	4175.	1380.	869.
97	1734.	3991.	1399.	979.
98	1931.	3876.	1411.	1109.
99	2211.	3713.	1431.	1249.
100	2526.	3563.	1448.	1440.
101	2894.	3412.	1468.	1600.
102	2538.	3592.	1446.	1560.
103	715.	5171.	1303.	423.
104	934.	4680.	1324.	591.
105	1136.	4337.	1357.	650.
106	1295.	4168.	1372.	759.
<u>50% urea solution</u>				
107	642.	4523.	1246.	444.
108	870.	4058.	1287.	570.
109	1040.	3813.	1302.	733.
110	1251.	3604.	1328.	882.
111	1473.	3424.	1349.	986.
112	1673.	3327.	1365.	1086.
113	1808.	3312.	1368.	1244.
114	667.	4511.	1262.	448.
115	884.	4080.	1298.	595.
116	1051.	3826.	1305.	804.
117	1229.	3677.	1333.	886.
118	1425.	3533.	1350.	997.
119	1667.	3428.	1367.	1137.
120	1860.	3343.	1375.	1295.

Table 5.6
 Comparison of Experimental Coefficients
 with those from Eqs.(2.74) and (2.76)(continued)

Run	Re	h from Eq.(2.74)	h from Eq.(2.76)	h in the present work
<u>50% urea solution</u>				
121	2248.	3230.	1397.	1558.
122	2101.	3358.	1387.	1422.
123	2028.	3451.	1379.	1384.
124	1867.	3572.	1364.	1259.
125	1627.	3725.	1344.	1118.
126	1372.	3940.	1323.	925.
<u>60% urea solution</u>				
127	870.	3999.	1231.	649.
128	1046.	3756.	1252.	794.
129	1181.	3596.	1268.	902.
130	1309.	3476.	1281.	998.
131	1415.	3386.	1289.	1124.
132	1508.	3313.	1299.	1159.
133	1672.	3219.	1312.	1316.
134	1763.	3170.	1317.	1390.
135	1535.	3332.	1298.	1234.
136	1416.	3428.	1289.	1109.
137	1301.	3526.	1278.	1020.
138	1209.	3624.	1270.	938.
139	1064.	3778.	1253.	838.
140	895.	3995.	1230.	719.
141	992.	3851.	1242.	786.
142	1029.	3800.	1248.	794.
143	1065.	3758.	1253.	828.
144	1100.	3696.	1257.	851.
145	1170.	3620.	1263.	927.
146	1222.	3567.	1266.	1030.



APPENDIX B

FIGURES (page 82-87)

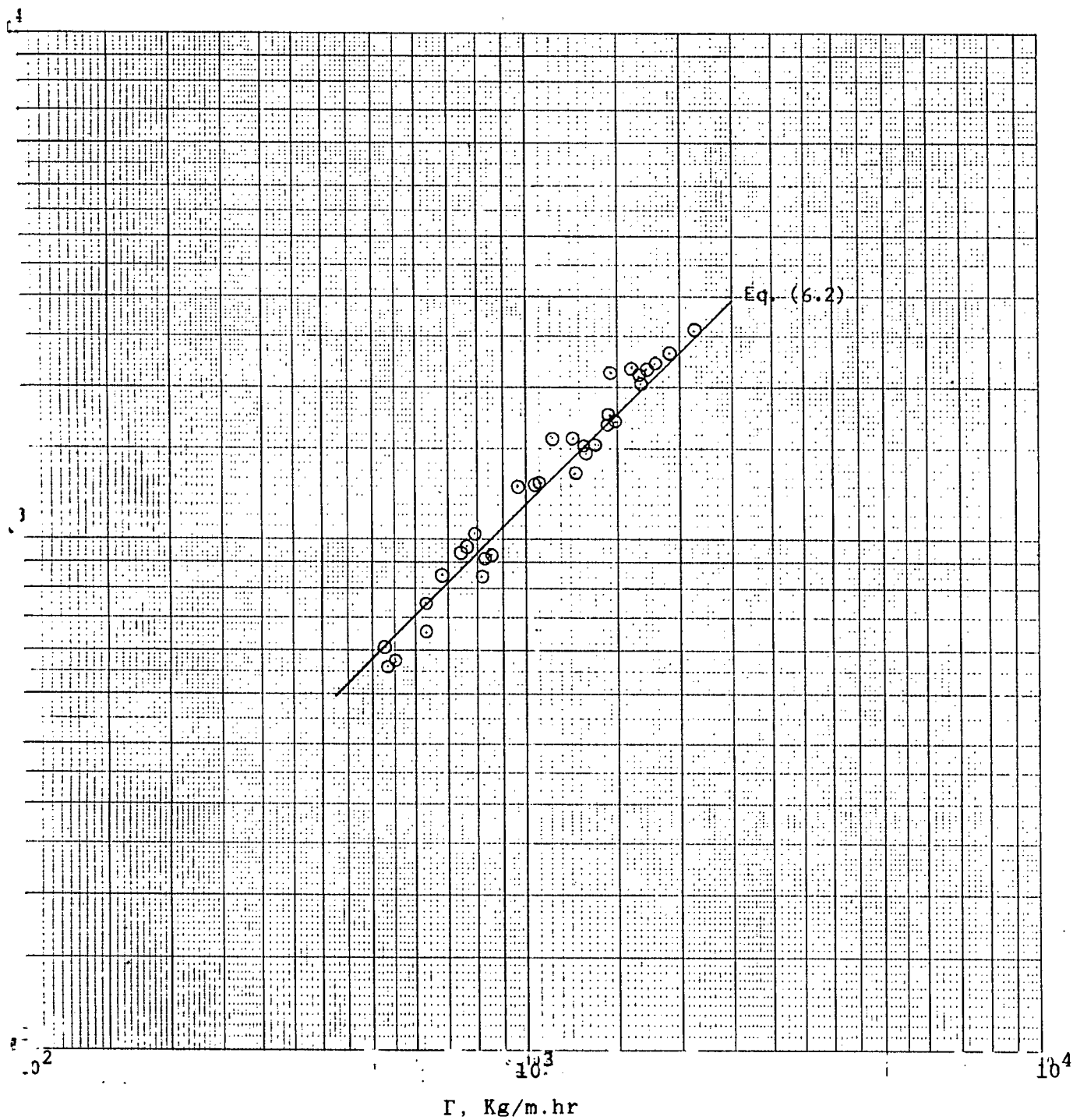


Figure 5.1 Film heat transfer coefficient vs. mass flow rate per unit width of the tube for water.

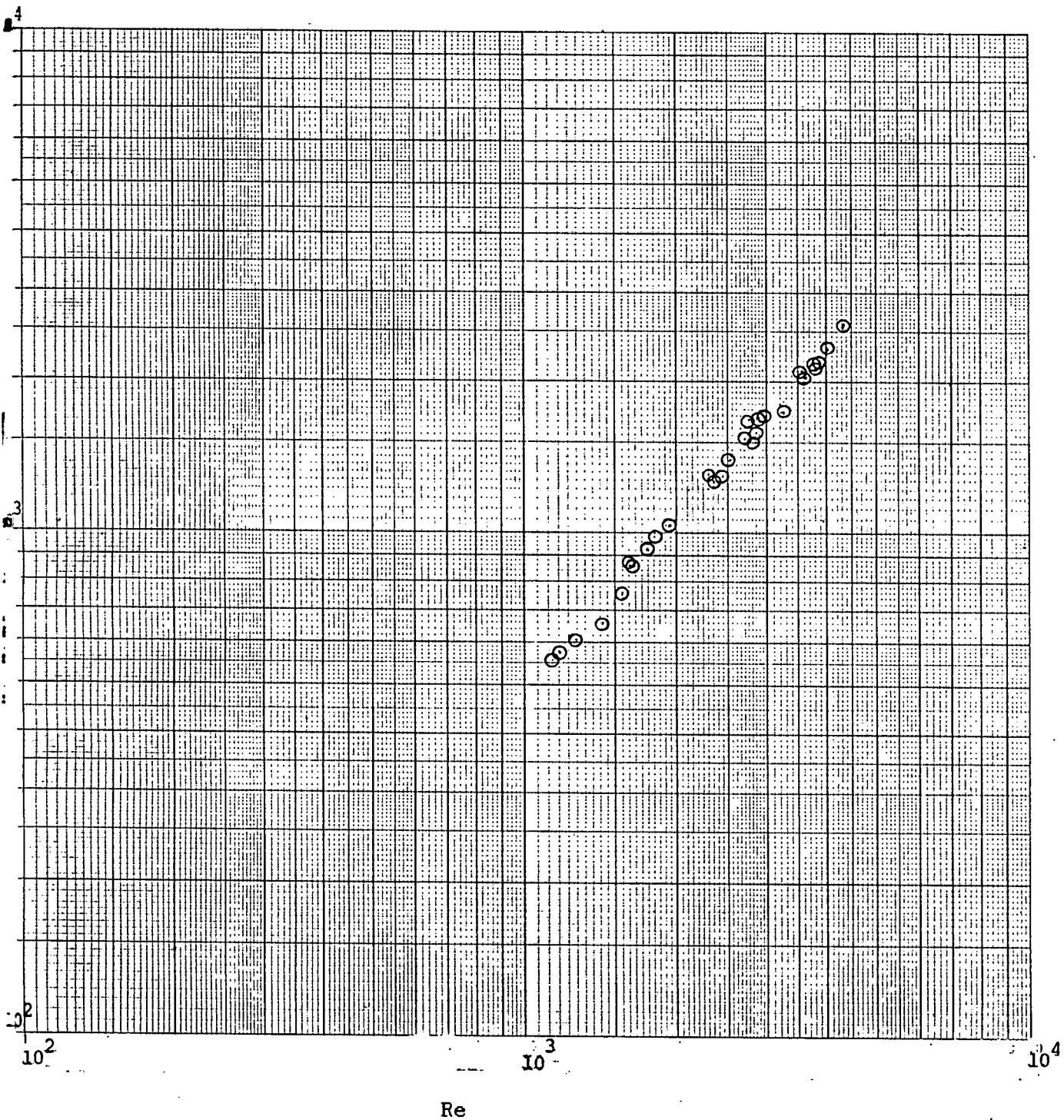
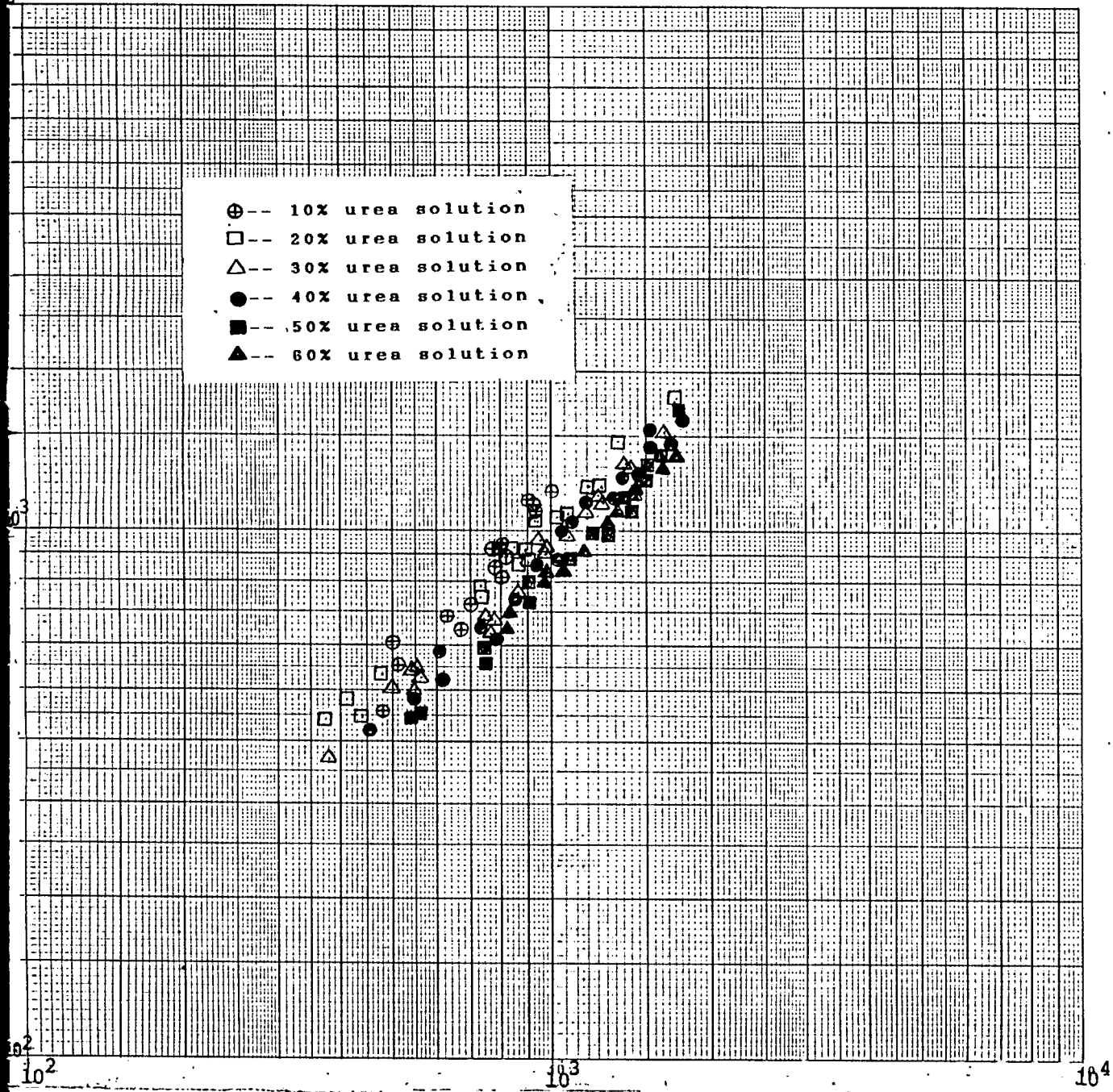


Figure 5.2 Film heat transfer coefficient vs. Reynolds number for water.

- ⊕-- 10% urea solution
- 20% urea solution
- △-- 30% urea solution
- 40% urea solution
- 50% urea solution
- ▲-- 60% urea solution



Γ , Kg/m.hr

Figure 5.3 Film heat transfer coefficient vs. mass flow rate per unit width of the tube for urea solutions.

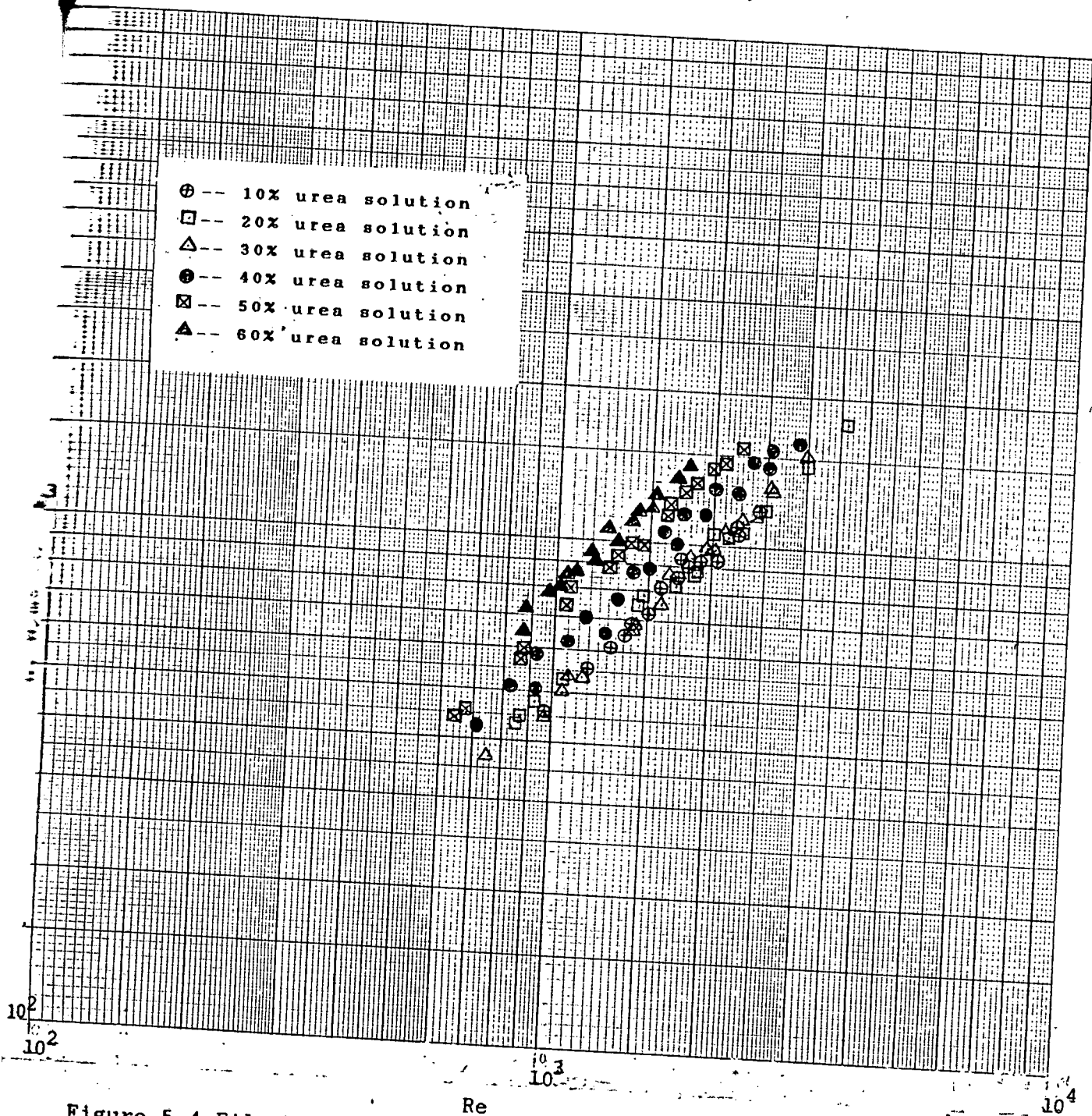


Figure 5.4 Film heat transfer coefficient vs. Reynolds number for urea solutions.

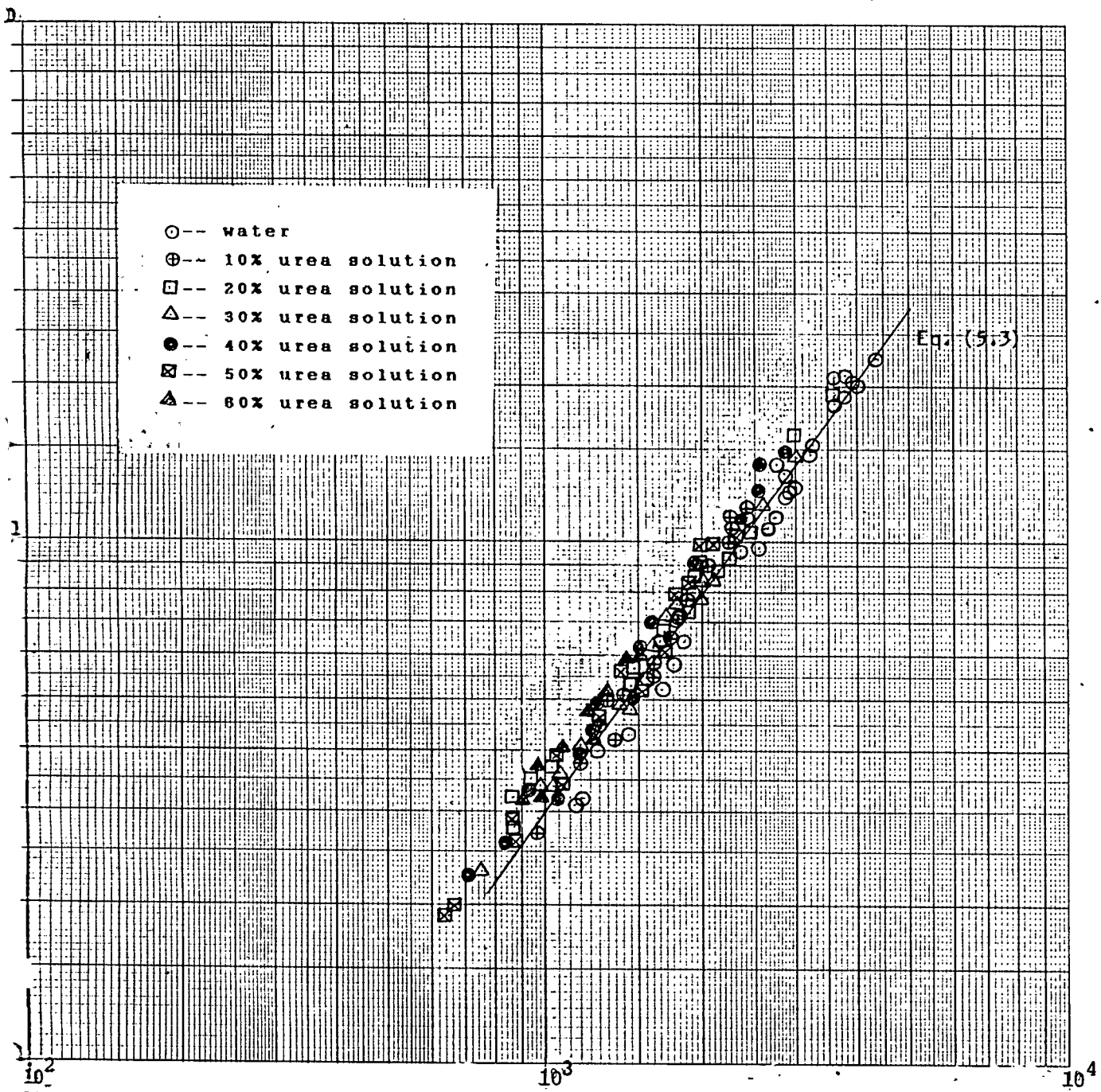


Figure 5.5 $Nu_{ext}/Pr^{1.71}$ vs. Reynolds number.

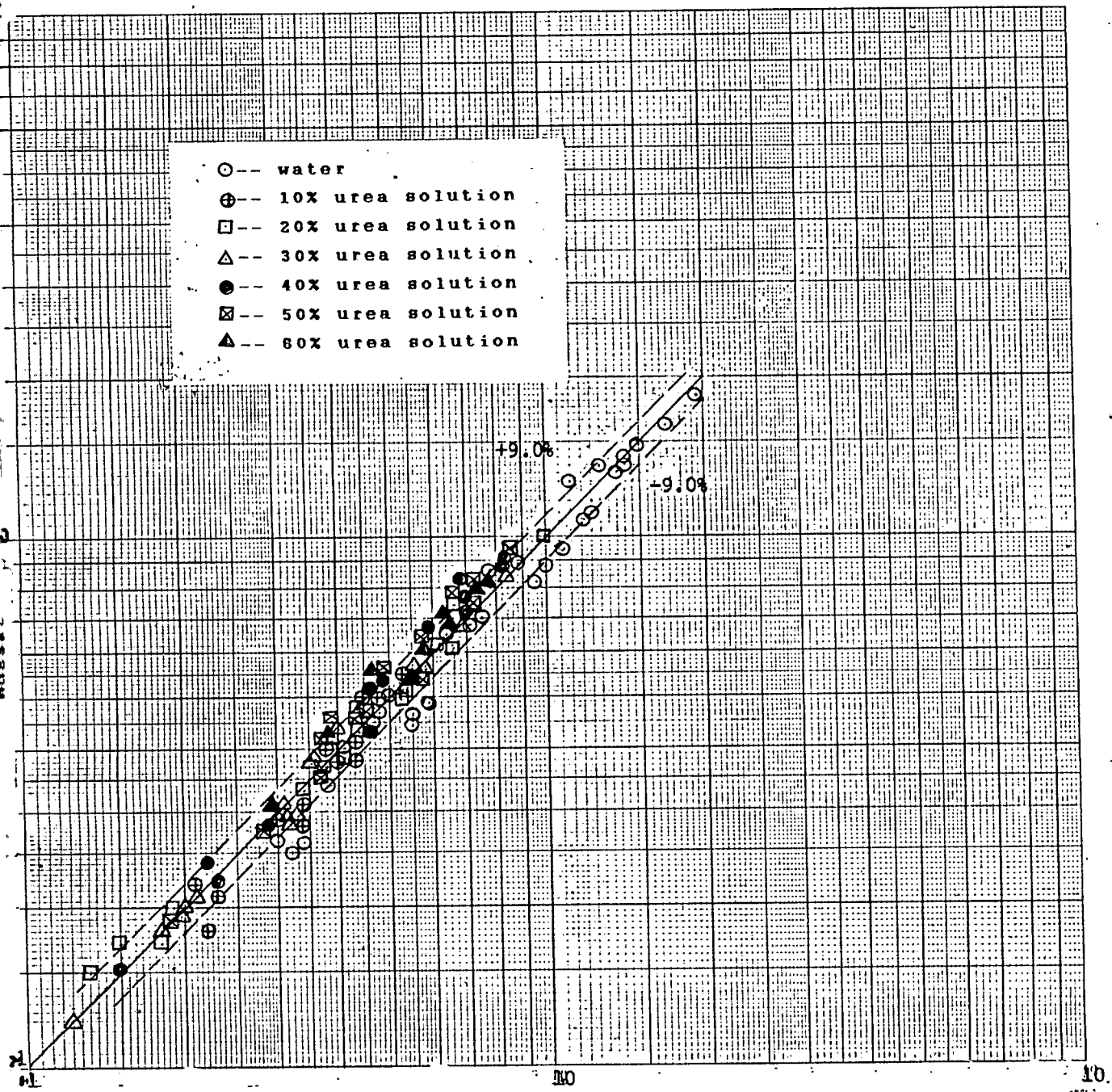


Figure 5.6 Experimental Nusselt number vs. calculated Nusselt number.

APPENDIX C

COMPUTER PROGRAM LISTINGS

PROGRAM-I calculates the heat transfer results for water and urea solutions. The results of PROGRAM-I are used in PROGRAM-II. PROGRAM-II do regression analysis.

```

***** PROGRAM-I *****
This program calculates the heat transfer results for water and
urea solution.
*****
***** Variable identification *****
NDATA= Total number of input data
INDEX= Quantity indicating the coc. of the solution
      INDEX=1 indicates pure water
      INDEX=2 indicates 10% urea solution
      INDEX=3 indicates 20% urea solution
      INDEX=4 indicates 30% urea solution
      INDEX=5 indicates 40% urea solution
      INDEX=6 indicates 50% urea solution
      INDEX=7 indicates 60% urea solution
      INDEX=8 indicates 70% urea solution
NRUN= Run number
NDT= Run number belonging to the solution type INDEX
DT= Tube diameter
LT= Tube length
MF= Mass flow rate, Kg/hr
TI= Inlet temp., C
TO= Outlet temp., C
TS= Steam temp., C
TA= Average liquid temp., C
TW= Average wall temp., C
TP= Corrected inside wall temp., C
QJ= Heat transfer, jacket side, W
QI= Heat transfer, tube side, W
QB= % Heat balance based on QJ
QA= Heat flux, W/m2
DTA= Average temp. difference, C
DTLM= Overall LMTD, C
WR= Peripheral liquid flow rate, Kg/hr.m
PR= Prandtl number at TA
REA= Reynolds number at TA
RET= Reynolds number at TP
NU= Nusselt number at TA
ST= Stanton numbr at AT
VISFAC= Viscosity correction factor
B= Film thickness, m
H= Film heat transfer coefficient W/m2. C
UI= Overall heat trasfer coefficient based on inside diameter
CP= Specific heat capacity of the liquid Cal/gm. C
K = Thermal conductivity of the liquid, W/m. C
DEN= Specific gravity of the liquid
VISCOA= Viscosity of the liquid at TA, cp
VISCOP= Viscosity of the liquid at TP, cp

```



```

PARAMETER(NDATA=146,INDEX=7)
IMPLICIT REAL*8 (A-H,O-Z)
REAL LT,MF,NU,NUVIS,K
DIMENSION WR(NDATA),TI(NDATA),TO(NDATA),TS(NDATA),TW(NDATA),
?TP(NDATA),TA(NDATA),DTA(NDATA),DTLM(NDATA),QI(NDATA),QJ(NDATA),
?QB(NDATA),QA(NDATA),PR(NDATA),REA(NDATA),REP(NDATA),H(NDATA),
?UI(NDATA),CP(NDATA),VISCOA(NDATA),VISCOF(NDATA),NDT(INDEX),
?ST(NDATA),B(NDATA),DEN(NDATA),VISFAC(NDATA),K(NDATA),
?NU(NDATA),NUVIS(NDATA),MF(NDATA),S(NDATA),HA(NDATA),FS(NDATA),
?HN(NDATA),HEXPT(NDATA),NUMC(NDATA),NUN(NDATA)
OPEN(UNIT=5,FILE='LIQ',STATUS='OLD')
OPEN(UNIT=6,FILE='COMP3',STATUS='NEW')
READ(5,11) DT,LT
READ(5,12)(NDT(J),J=1,INDEX)
DO 200 I=1,NDATA
READ(5,13) NRUN,MF(I),TI(I),TO(I),TW(I),TS(I),QJ(I),CP(I),
?DEN(I),K(I)
200 CONTINUE
11 FORMAT(2F7.5)
12 FORMAT(7I2)
13 FORMAT(I3,F6.1,4F5.1,F8.1,F5.2,F5.3,F6:4)
*
* Calculate heat transfer in the tube side
*
DO 210 I=1,NDATA
QI(I)=MF(I)*CP(I)*(TO(I)-TI(I))*1.8
210 CONTINUE
*
* Calculate % heat balance and heat flux and corrected wall temp.
*
DO 220 I=1,NDATA
QB(I)=(QJ(I)-QI(I))/QJ(I)*100.0
QA(I)=(QI(I)+QJ(I))/(2.*3.414*DT*LT)
TP(I)=TW(I)-2.9085E-04*QA(I)
220 CONTINUE
*
* Calculate average liquid temp, avg. temp. diff. and overall LMTD
*
DO 230 I=1,NDATA
TA(I)=(TI(I)+TO(I))/2.0
DTA(I)=TP(I)-TA(I)
DTLM(I)=((TS(I)-TI(I))-(TS(I)-TO(I)))/
? DLOG((TS(I)-TI(I))/(TS(I)-TO(I)))
230 CONTINUE
* Calculate viscosity of the liquid from correlation
N=1
NDT1=NDT(1)

```

```

DO 280 J=1,INDEX
  DO 290 I=N,NDT1
    GOTO(31,32,33,34,35,36,37,38),J
31    VISCOA(I)=1.37248*DEXP(-0.01661*TA(I))
      VISCOP(I)=1.37248*DEXP(-0.01661*TP(I))
      GOTO 290
32    VISCOA(I)=1.09730*DEXP(-0.01272*TA(I))
      VISCOP(I)=1.09730*DEXP(-0.01272*TP(I))
      GOTO 290
33    VISCOA(I)=1.21126*DEXP(-0.01274*TA(I))
      VISCOP(I)=1.21126*DEXP(-0.01274*TP(I))
      GOTO 290
34    VISCOA(I)=1.40636*DEXP(-0.01332*TA(I))
      VISCOP(I)=1.40636*DEXP(-0.01332*TP(I))
      GOTO 290
35    VISCOA(I)=1.62229*DEXP(-0.01250*TA(I))
      VISCOP(I)=1.62229*DEXP(-0.01250*TP(I))
      GOTO 290
36    VISCOA(I)=1.96925*DEXP(-0.01205*TA(I))
      VISCOP(I)=1.96925*DEXP(-0.01205*TP(I))
      GOTO 290
37    VISCOA(I)=2.13886*DEXP(-0.00939*TA(I))
      VISCOP(I)=2.13886*DEXP(-0.00939*TP(I))
      GOTO 290
38    VISCOA(I)=2.95999*DEXP(-0.00900*TA(I))
      VISCOP(I)=2.95999*DEXP(-0.00900*TP(I))
290  CONTINUE
      N=NDT1+1
      NDT1=NDT1+NDT(J+1)
280  CONTINUE
*
* Calculate peripheral liquid flow rate, Reynolds number at TA
* and Reynolds number at TP
*
  DO 240 I=1,NDATA
    WR(I)=MF(I)/(3.1414*DT)
    REA(I)=4.0*WR(I)/(VISCOA(I)*2.42)
    REP(I)=4.0*WR(I)/(VISCOP(I)*2.42)
240  CONTINUE
*
* Calculate film heat transfer coefficient h, and overall heat
* transfer coefficient, Ui
*
  DO 250 I=1,NDATA
    H(I)=QA(I)/(DTA(I)*1.8)
    UI(I)=QA(I)/(DTLM(I)*1.8)

```

250 CONTINUE

```
*
* Calculate film thickness
*
  DO 260 I=1,NDATA
    DEN(I)=(DEN(I)*62.4)**2
    B(I)=(3.*VISCOA(I)*2.42*WR(I)/(DEN(I)*414.72E+06))**.3333
```

260 CONTINUE

* Calculate Nusselt number, Prandtl number, Stanton number and

* viscosity correction factor

```
*
  DO 270 I=1,NDATA
    PR(I)=CP(I)*VISCOA(I)*2.42/K(I)
    NU(I)=H(I)*B(I)/K(I)
    ST(I)=NU(I)/(REA(I)*PR(I))
    VISFAC(I)=(VISCOA(I)/VISCOPI(I))**.25
    NUVIS(I)=NU(I)/VISFAC(I)
```

270 CONTINUE

* Calculate h using Nusselt's theoretical equation

```
  DO 401 I=1,NDATA
    S(I)=K(I)*VISCOA(I)*2.42*6.5
    S(I)=S(I)/(B(I)**4*DEN(I)*CP(I)*414720000.)
    IF(S(I).LT.0.05) FS(I)=2.230*S(I)**0.656
    IF(S(I).GT.0.05) FS(I)=1.-0.9101*DEXP(-5.65*S(I))
    HN(I)=WR(I)*CP(I)*DLOG(1./(1.-FS(I)))/6.5
```

401 CONTINUE

* Calculate h using McAdams equation

```
  DO 410 I=1,NDATA
    HA(I)=2.1*CP(I)*WR(I)*VISFAC(I)*S(I)**.667/6.5
```

410 CONTINUE

* Calculate h using Experimental correlation

```
  DO 420 I=1,NDATA
    HEXPT(I)=0.0000043*K(I)*REA(I)**1.30*PR(I)**1.71/B(I)
```

420 CONTINUE

* Unit conversion from FPS to SI

```
  DO 320 I=1,NDATA
    MF(I)=MF(I)*(0.45359)
    WR(I)=WR(I)*(1.4882)
    H(I)=H(I)*0.00568*1000.
    UI(I)=UI(I)*0.00568*1000.
    QI(I)=QI(I)*0.00029307*1000.
    QJ(I)=QJ(I)*0.00029307*1000.
    QA(I)=QA(I)*0.0031546*1000.
    HN(I)=HN(I)*0.00568*1000.
    HA(I)=HA(I)*0.00568*1000.
    HEXPT(I)=HEXPT(I)*0.00568*1000.
    NUMC(I)=HA(I)*B(I)/K(I)
    NUN(I)=HN(I)*B(I)/K(I)
```

```

320 CONTINUE
*
* Print results
*
* WRITE(6,3001)
  N=1
  NDT1=NDT(1)
  DO 300 J=N,INDEX
    L=J-1
*       WRITE(6,3005) L
*       WRITE(6,3001)
*       WRITE(6,3007)

    DO 310 I=N,NDT1
*       WRITE(6,3006) I,WR(I),NU(I),REA(I),PR(I),ST(I),NUVIS(I),H(I)
*       WRITE(6,3002) I,MF(I),TI(I),TO(I),TW(I),TS(I),QI(I),
*       ?           QJ(I),QB(I),QA(I),TP(I),DTA(I),DTLM(I)
*       WRITE(6,3008) MF(I),WR(I),H(I),UI(I),NU(I),REA(I),PR(I)
*       WRITE(6,3012) I,REA(I),HN(I),HA(I),H(I)
*       WRITE(6,3011) I,NU(I),NUMC(I),NUN(I),NUCALC(I)
310 CONTINUE
  N=NDT1+1
  NDT1=NDT1+NDT(J+1)
300 CONTINUE
3005 FORMAT(I1,'0 wt% urea solution'/21(1H-))
3001 FORMAT(T4,'Mass',T14,'Fluid Temp.C',T27,'Avg.',T36,'Steam',
?T63,'% ',T68,'Heat',T77,'Corrected',T87,'Avg.',T97,'Overall',
?/T4,'Flow',T14,'-----',T27,'wall',T36,'Temp.',T46,'Qi',
?T54,'Qj',T60,'Heat',T68,'Flux',T77,'Wall Temp.',T87,'Temp.',
?T97,'Log mean'/Run',T4,'Rate',T14,'Ti      To',T27,'Temp.',
?T87,'Diff.',T97,'Temp.diff.C'/T4,'Kg/hr',T27,'Tw C',T36,'Ts C',
?T44,'W',T52,'W',T60,'Balance',T68,'W/m ',T77,
?'Tp C',T87,' T C',T97,' Tlm C'/)
3002 FORMAT(I3,1X,F7.1,1X,F5.1,2X,F5.1,1X,F6.1,1X,F7.1,1X,F7.0,1X,
?F7.0,1X,F7.2,1X,F8.0,1X,F8.1,1X,F8.1,1X,F8.1)
3006 FORMAT(2X,I3,4(F10.2),E10.3,F10.3,F10.2/2X,73(1H-))
3007 FORMAT(/2X,73(1H=)/2X,'Run',7X,'Wr',8X,'Nu',8X,'Re',8X,'Pr',8X,
?'St',7X,'Nuvis',6X,'h'/2X,73(1H=))
3008 FORMAT(7F10.2)
3012 FORMAT(5X,I3,4(2X,F8.0))
  STOP
  END

```

***** PROGRAM II *****

PARAMETER (NDATA=146,M=3,N=4)

REAL NNU(NDATA),NRE(NDATA),NPR(NDATA),NUD(NDATA),

1 NUCALC(NDATA),NU(NDATA),NUDD(NDATA),NUPR(NDATA),

2 MF(NDATA),WR(NDATA),H(NDATA),U(NDATA)

COMMON/PP/X(NDATA),Y(NDATA),Z(NDATA)

OPEN(UNIT=5,FILE='FILM',STATUS='OLD')

OPEN(UNIT=6,FILE='WF1',STATUS='NEW')

101 FORMAT(7F10.2)

DO 440 I=1,NDATA

 READ(5,101) MF(I),WR(I),H(I),U(I),NNU(I),NRE(I),NPR(I)

440 CONTINUE

CALL REGRN(NNU,NRE,NPR,MF,WR,H,U)

STOP

END

SUBROUTINE REGRN(NNU,NRE,NPR,MF,WR,H,U)

* This Subroutine fits a regression equation of Nusselt Number(NNU), *

* Reynolds Number(NRE) and Prandtl Number. *

* NNU=Function of(NRE and NPR) *

* *

***** Variable identification *****

* NDATA= Number of data *

* NNU = Nusselt Number *

* NRE = Reynolds Number *

* NPR = Prandtl Number *

* *

***** Storage Allocation *****

* *

PARAMETER(NDATA=146,M=3,N=4)

REAL NNU(NDATA),NRE(NDATA),NPR(NDATA),NUD(NDATA),NU(NDATA),

1 NUCALC(NDATA),NUDD(NDATA),NUPR(NDATA),MF(NDATA),WR(NDATA),

2 H(NDATA),U(NDATA)

COMMON/PP/ X(NDATA),Y(NDATA),Z(NDATA)

DIMENSION A(M,N),C(M)

* *

* Calculate logarithms of NNU,NPR and NRE-values *

* *

DO 401 I=1,NDATA

 Z(I)=ALOG(NNU(I))

 X(I)=ALOG(NRE(I))

 Y(I)=ALOG(NPR(I))

* *

401 CONTINUE

```

*
* Initialization block
*
    SUMX=0.
    SUMY=0.
    SUMZ=0.
    SUMXX=0.
    SUMXY=0.
    SUMYY=0.
    SUMYZ=0.
    SUMZX=0.
*
* Generate Matrix elements
*
    DO 402 I=1,NDATA
        SUMX=SUMX+X(I)
        SUMY=SUMY+Y(I)
        SUMZ=SUMZ+Z(I)
        SUMXX=SUMXX+X(I)*X(I)
        SUMXY=SUMXY+X(I)*Y(I)
        SUMYY=SUMYY+Y(I)*Y(I)
        SUMYZ=SUMYZ+Y(I)*Z(I)
        SUMZX=SUMZX+Z(I)*X(I)
402 CONTINUE
*
* Arrange the Matrix elements
*
    A(1,1)=NDATA
    A(1,2)=SUMX
    A(1,3)=SUMY
    A(1,4)=SUMZ
    A(2,1)=SUMX
    A(2,2)=SUMXX
    A(2,3)=SUMXY
    A(2,4)=SUMZX
    A(3,1)=SUMY
    A(3,2)=SUMXY
    A(3,3)=SUMYY
    A(3,4)=SUMYZ
*
* Call Subroutine SIMUL, to solve simultaneous linear equations
*
    CALL SIMUL(A,C)
*
* Coefficiens of Regression equation
*

```

```

A1=EXP(C(1))
A2=C(2)
A3=C(3)
*   WRITE(6,3001) A1,A2,A3
3001 FORMAT(/10X,'The required correlation is', ' Nu=',F10.7,'*(NRe**',
1     F6.4,')*(NPr**',F6.4')')
DO 409 I=1,NDATA
      NUPR(I)=NNU(I)/(NPR(I)**A3)
409  CONTINUE
*
*   Calculate the values of Nu from the correlation
*
      WRITE(6,3002)
DO 403 I=1,NDATA
      NUCALC(I)=A1*NRE(I)**A2*NPR(I)**A3
      WRITE(6,3003) I,MF(I),WR(I),H(I),U(I),NRE(I),NPR(I),
?     NNU(I),NUCALC(I),NUPR(I)
*   WRITE(6,3020) WR(I),H(I)
403  CONTINUE
3002 FORMAT(T5,'Mass',T14,'Peripheral'/T4,'Flow rate',T14,'Mass Flow',
?/'Run',T5,'mf',T14,'Rate',T30,'h',T45,'U1',T55,'Re',T63,'Pr',
?T69,'Nu',T84,'Nucalc',T93,'Nu/Pr'/T5,'Kg/hr',T14,'Kg/hr.m',
?T27,'W/m2 C',T40,'W/m2 C'/)
3003 FORMAT(I3,1X,F7.1,1X,F10.1,1X,F8.1,1X,F8.1,1X,F8.0,1X,F4.1,1X,
?F6.1,1X,F6.1,1X,F6.2)
3020  FORMAT(2F10.2)
*
*   Calculate Standard error of estimate
*
      SNUD=0.
DO 404 I=1,NDATA
      NUD(I)=NNU(I)-NUCALC(I)
      SNNUD=SNNUD+NUD(I)**2
404  CONTINUE
      SD=SNNUD/(NDATA-1)
*
*   Calculate Standard Deviation
*
      SNU=0.
DO 405 I=1,NDATA
      SNU=SNU+NNU(I)
405  CONTINUE
      SNUBAR=SNU/NDATA
      SNUD=0.
DO 406 I=1,NDATA
      NUDD(I)=NNU(I)-SNUBAR

```



```

*
*****
*
***** Storage Allocation *****
*
  PARAMETER(M=3,N=4)
  DIMENSION A(M,N),C(M)
*
* Select PIVOT element
*
  DO 411 K=1,M
    PIVOT=A(K,K)
*
* Checks that PIVOT row element is non-zero
*
    IF(ABS(PIVOT).LE.0.0001) GOTO 20
*
* Normalizes PIVOT row
*
    DO 412 J=K,N
      A(K,J)=A(K,J)/PIVOT
412 CONTINUE
* Zeros PIVOT column
*
    DO 413 I=1,M
      IF(I.EQ.K) GOTO 413
      PIVI=A(I,K)
      DO 414 J=K,N
        A(I,J)=A(I,J)-PIVI*A(K,J)
414 CONTINUE
413 CONTINUE
411 CONTINUE
*
* Set up a solution vector C(i,j)
*
  DO 415 J=1,M
    C(J)=A(J,N)
415 CONTINUE
  RETURN
*
* Error comment
*
20 WRITE(6,3000) K
3000 FORMAT(10X,'Pivot element',I2,' is close to zero'/)
  RETURN
  END

```